ANALYSES OF DYKE SWARMS WITHIN THE SVERDRUP BASIN QUEEN ELIZABETH ISLANDS

Submitted by: Wayne Jollimore

In Partial Fulfillment of BSc Honours Degree

Supervisor: G.K. Muecke

March 7, 1986

Distribution License

DalSpace requires agreement to this non-exclusive distribution license before your item can appear on DalSpace.

NON-EXCLUSIVE DISTRIBUTION LICENSE

You (the author(s) or copyright owner) grant to Dalhousie University the non-exclusive right to reproduce and distribute your submission worldwide in any medium.

You agree that Dalhousie University may, without changing the content, reformat the submission for the purpose of preservation.

You also agree that Dalhousie University may keep more than one copy of this submission for purposes of security, back-up and preservation.

You agree that the submission is your original work, and that you have the right to grant the rights contained in this license. You also agree that your submission does not, to the best of your knowledge, infringe upon anyone's copyright.

If the submission contains material for which you do not hold copyright, you agree that you have obtained the unrestricted permission of the copyright owner to grant Dalhousie University the rights required by this license, and that such third-party owned material is clearly identified and acknowledged within the text or content of the submission.

If the submission is based upon work that has been sponsored or supported by an agency or organization other than Dalhousie University, you assert that you have fulfilled any right of review or other obligations required by such contract or agreement.

Dalhousie University will clearly identify your name(s) as the author(s) or owner(s) of the submission, and will not make any alteration to the content of the files that you have submitted.

If you have questions regarding this license please contact the repository manager at dalspace@dal.ca.

Grant the distribution license by signing and dating below.

_____ _____

Name of signatory Date

ANALYSES OF DYKE SWARMS WITHIN THE SVERDRUP BASIN QUEEN ELIZABETH ISLANDS

ABSTRACT

The Sverdrup Basin is a sedimentary basin within the Canadian Arctic Islands. This area has had a complex tectonic and igneous history with several episodes of intrusive and extrusive activity. The last episode is believed to have occurred in two stages during the Cretaceous. The first stage resulted in the emplacement of dykes along a trend sub-parallel to the axis of the basin. The second produced a trend in a north-south direction and is believed to represent the landward continuation of the Alpha Ridge complex. The petrology and geochemistry of the north-trending swarm is examined and a brief comparison is made with the Strand Fiord Formation Volcanics.

TABLE OF CONTENTS

LIST OF FIGURES

LIST OF PLATES

LIST OF TABLES

ACKNOWLEDGEMENTS

The author would like to thank Dr. Muecke of Dalhousie University for his time and effort spent reviewing the text, and for the helpful suggestions and comments he made to help improve it. It is most appreciated.

The author would also like to thank Ms. Marie-Claude Williamson for taking time out of her busy schedule to help whenever it was required.

Last, but far from least, the author wishes to thank Miss Lisa Henderson for typing the text and for helping with the final drafting and assembly of the document.

CHAPTER 1

INTRODUCTION AND BACKGROUND

CHAPTER 1

INTRODUCTION AND BACKGROUND

1.1 Introduction

The Sverdrup Basin is a sedimentary basin occupying the central part of the Queen Elizabeth Islands in Canada's Arctic (Figure 1a). This area has had a long and complex geologic history with several deformational episodes and extensive igneous activity. The lithology of the basin consists of marine and non-marine clastics, carbonates and evaporites with ages ranging from Lower Carboniferous to Tertiary. Basaltic dykes, sills and extrusive volcanics are widespread within the basin and have been emplaced in several distinct pulses. Little is known about the timing of the intrusive pulses and their relationship to the extrusive volcanics in the stratigraphic section. The nature and timing of the igneous activity are of considerable interest in studies of the extension and evolution of the Sverdrup Basin. The mechanism that caused the extension of the Sverdrup Basin may also be responsible for the formation of the Canada Basin and Alpha Ridge Complex (Figure 1b).

Regional mapping by the G.S.C. on a scale of 1:250,000 has been completed over most of the basin and reveals abundant dykes in many parts. Even casual inspection shows that the dykes are unevenly distributed and show several preferred directions. To

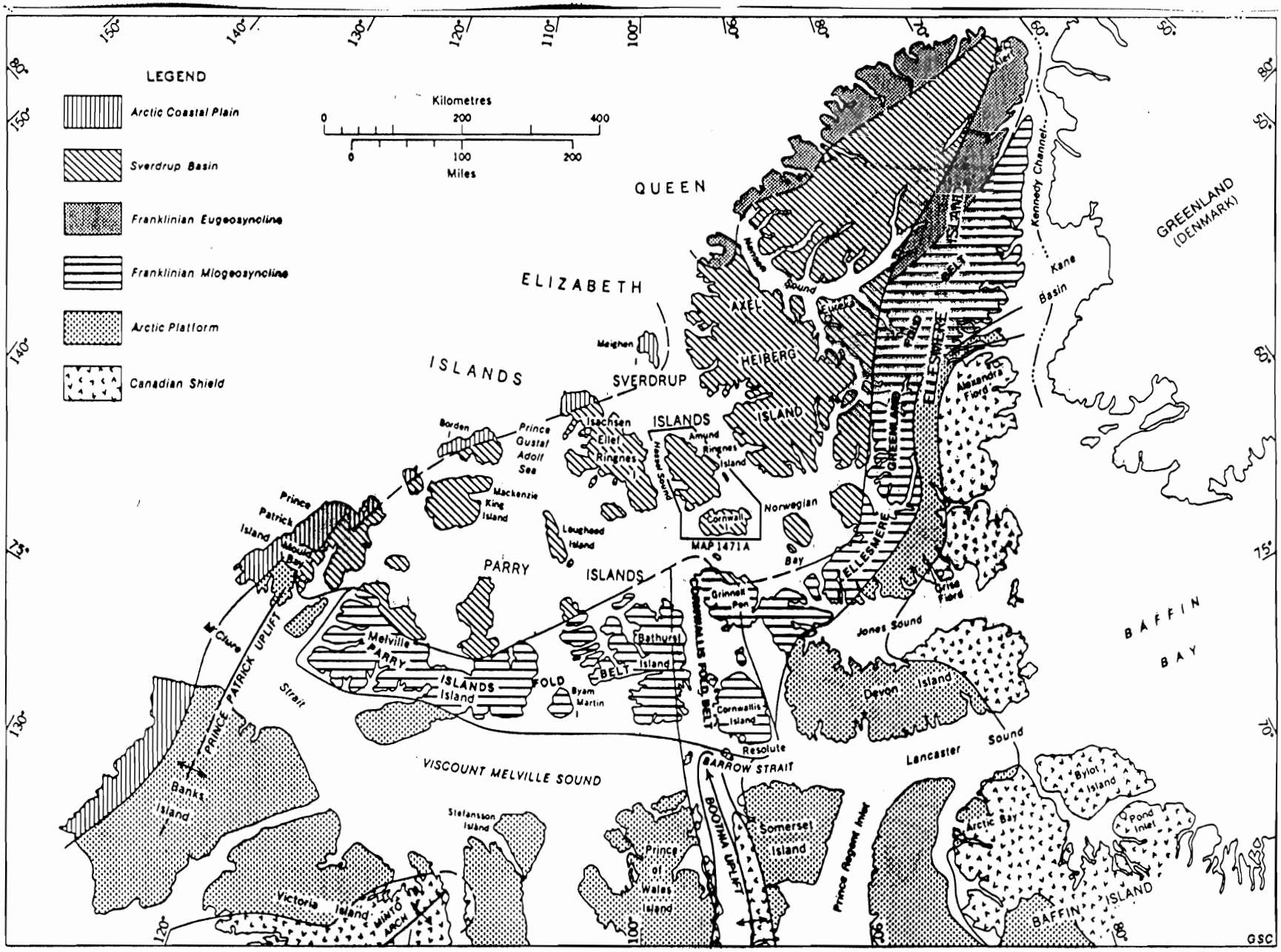

Figure 1a: Geological Provinces, Queen Elizabeth Islands (after Thorsteinsson and Tozer, 1970.)

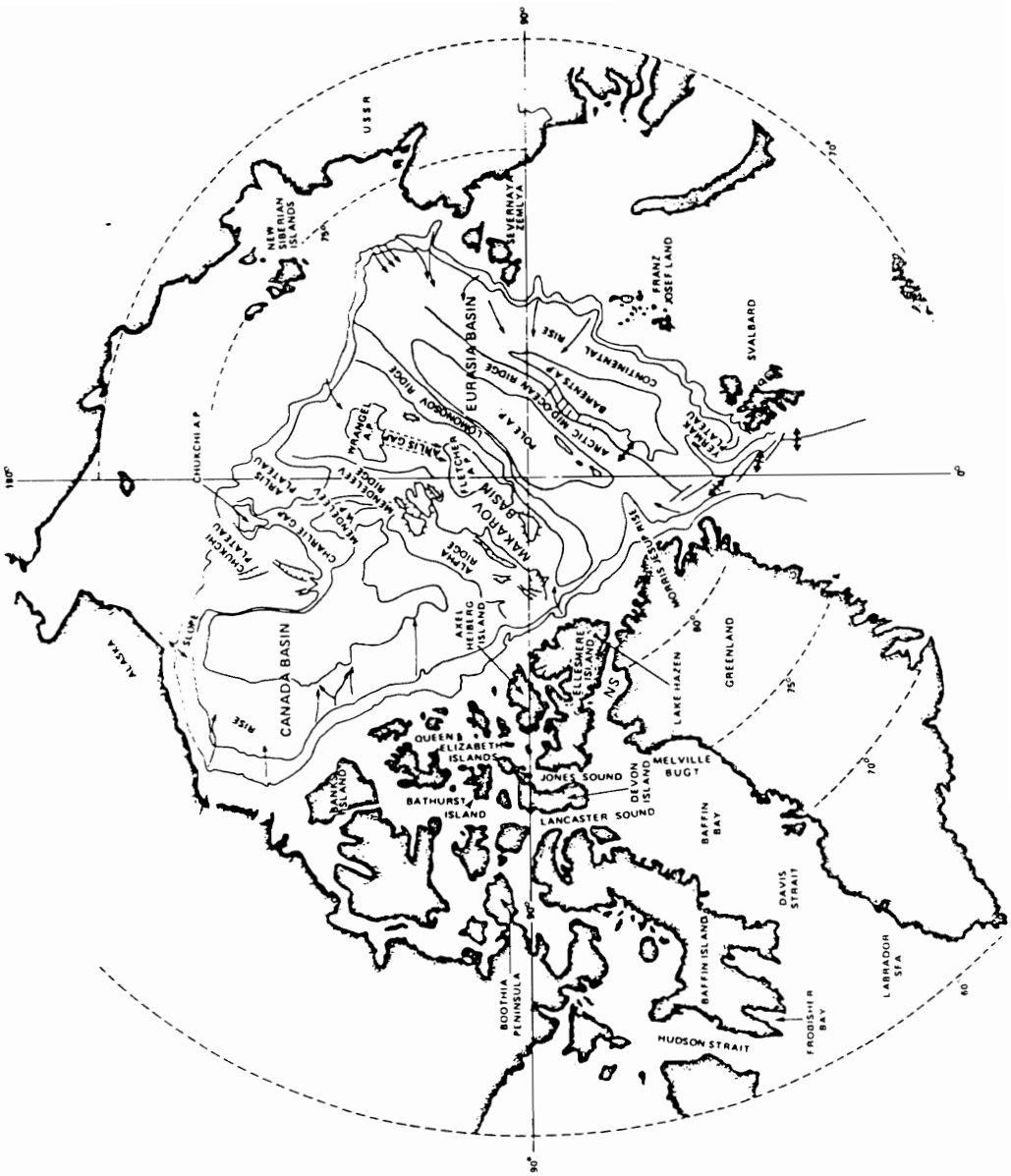

Figure 1b: Index Map of Arctic Islands, Adjacent Alpha Ridge and Canada Basin

date, no systematic analysis of the dyke swarm(s) has been undertaken. The dyking is important in understanding the later stages of extension within the basin and possibly the subsequent development of hydrocarbons. Extension and igneous activity would tend to elevate the geothermal gradient of the basin which will affect maturation of organic materials and the production of oil and gas.

Only dykes are used in this study because they are shown on maps, whereas the sills are not. Sills are extremely common in the central portions of the basin and may be volumetrically more abundant than the dykes (G. Muecke, pers. com.). The purpose of this study is to:

- determine the distribution of dykes and the frequency of occurrence over the basin,

- determine the orientation and preferred dyking directions within the basin,

- establish whether there is more than one episode of dyking and the relative timing of these events,

- stratigraphically bracket individual swarms, and where possible, to correlate these with known age dates and extrusive events,

- to examine the petrology and geochemistry of one of the dyke swarms in the Lightfoot River area on Axel Heiberg Island.

1.2 Previous Work

The Canadian Arctic Islands have been the subject of intense geological work since the early 1960's.

Stratigraphic work was begun by Thorsteinsson and Tozer (1960). This was followed up with more work by Thorsteinsson and Tozer (1970), Thorsteinsson (1971a, 1971b, 1974), Trettin and Hills (1966), and Trettin et al. (1972). Other workers that have studied the stratigraphy include Embry and Klovan (1976), Embry (1982, 1983a, 1983b), Balkwill et al. (1977), Balkwill and Fox (1982), and Balkwill (1983a, 1983b).

Models for the evolution of the Sverdrup Basin have been proposed by Sweeney et al. (1978), Balkwill (1978), and Kerr (1980).

Blackadar (1964) began petrographic work on the basic igneous rocks within the basin. This has been followed up by Osadetz (1982), Osadetz and Moore (in press); Ricketts et al. (1985), and Williamson (PhD Thesis Dalhousie University in preparation).

Gravity surveys were carried out over the Sverdrup Basin by Sobczak (1963). Later, Sobczak and Weber (1970) used geophysics to determine the nature of the basement rock and structure, and also to determine the depth to the mantle. Jackson and Halls

(1983) undertook a paleomagnetic survey of igneous rocks in the Sverdrup Basin, following an earlier survey by Larochelle et al. (1965).

Much work is also being carried out in the adjacent Canada Basin and Alpha Ridge complex. Vogt and Ostenso (1970) have done magnetic and gravity profiles across the Alpha Ridge to determine its relationship to Arctic sea-floor spreading. Ostenso and Wold (1977) have done seismic and gravity profiles across the Arctic Ocean Basin. Jackson et al. (in press) have been studying the Alpha Ridge using seismics and drill core data.

1.3 Regional Setting

The Arctic Islands are bordered by the Arctic Ocean Basin to the northwest, the North American continental plate to the south, and is separated by the Nares Strait suture zone from Greenland to the east.

The Sverdrup Basin is a structural depression within the Canadian Arctic Islands. Basement consists of granites and metamorphic rocks of the Canadian Shield. K-Ar age determination yields ages of about 1.7 b.y. (Balkwill, 1978) for these rocks. Proterozoic and Lower Paleozoic clastics and carbonates unconformably overlie basement rocks, and are called the Arctic Platform. Above this lies a sequence known as the Franklinian Geosyncline. It includes: the Pearya geanticline, which at times in the past was an important source of clastic materials;

Hazen trough, which was a submarine foredeep, trending southwest; and a wedge of clastic and carbonate rocks believed to have accumulated between the Arctic platform and Hazen trough. These rocks were locally intruded and metamorphosed, and folded and faulted by the Middle Devonian to Upper Carboniferous Ellesmerian orogeny. Unconformably overlying this succession are Lower Carboniferous to Upper Tertiary marine, non-marine and evaporite strata with maximum thicknesses of up to 13,000 m. (Balkwill, 1978). Abundant dykes and sills cut all these strata, and locally extrusives occur within the Sverdrup Basin sequence. These rocks, in turn have been deformed by the Lower Cretaceous to Middle Tertiary Eurekan orogeny.

1.4 Tectonic and Igneous History

The tectonic history of the Arctic region is very complex and is just beginning to be understood. Prior to the Devonian the Arctic Islands were part of the North American Plate. The Middle Devonian through to the Early Carboniferous marked an extensive episode of mountain building and pluton injection known as the Ellesmerian orogeny. This episode affected the whole of the Arctic Islands and produced strong structural trends in the basement and overlying rocks. The directions of these trends varied from location to location. Northerly to northeasterly trends were formed in Ellesmere and Axel Heiberg Islands. These changed to more easterly along the southern margin of the Arctic

Islands. These trends consisted of folding and faulting of the rocks involved in the orogeny and possibly shearing deeper in the basement rocks.

The Boreal Rifting Episode began in the Late Devonian. Extension caused crustal thinning of the basement beneath the future Sverdrup Basin and this led to subsidence of the area and subsequent basin development. During the extension and subsidence of the basin, there were several episodes of intrusive (dykes and sills) and extrusive activity, one in the Upper Carboniferous, another in the Lower Permian, and several in the Lower and Upper Cretaceous. Figure 2 shows the stratigraphic position of extrusive flows within the basin and ages of intrusive rocks that have been dated. The latest episodes, in the Lower and Upper Cretaceous occurred at the same time as the formation of the Alpha Ridge. This suggests that the mechanism that was responsible for the extension of the Sverdrup Basin may have also been responsible for the rifting of the Alpha Ridge. This extension is also believed to have caused the block of crust containing the Arctic Islands to break away from the rest of the continent (Kerr, 1980).

The Late Cretaceous to Middle Tertiary Eurekan Deformation began to affect the area east of the Arctic Islands as the Boreal Rifting slowed. This event caused rifting of Baffin Bay and Davis Strait, and compressional deformation along the boundary between Northwest Greenland and Ellesmere Island (Jackson, 1985). In the Baffin Bay and Davis Strait areas this event was

accompanied by intrusive and extrusive basaltic volcanism (Clarke 1969, 1970, 1975, Clarke, Muecke, Pe-Piper 1983). The effect of this event was to cause regional uplift of the Sverdrup Basin and regional compression along the eastern margins of the basin (Balkwill, 1978). No igneous activity seems to have accompanied this event in the Sverdrup Basin. Towards the Middle Tertiary, this too became dormant as spreading activity shifted to its present location the Mid-Atlantic Ridge.

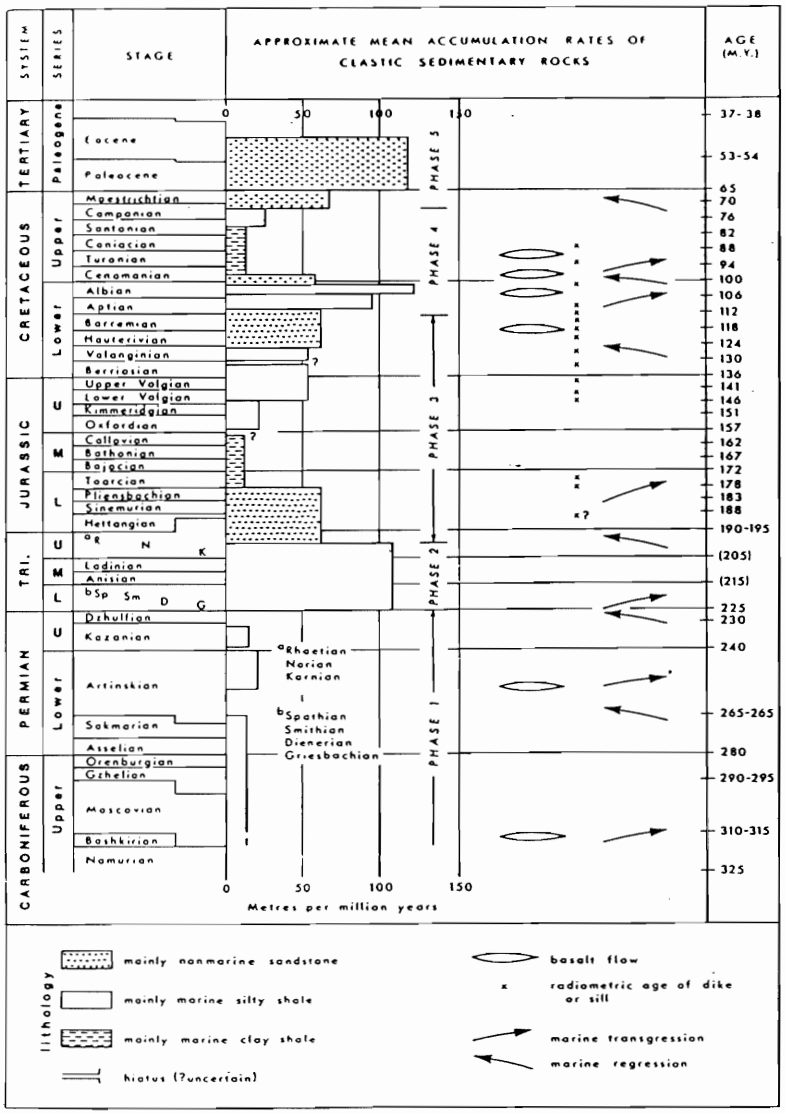

Figure 2: Sediment Accumulation Rates and Stratigraphic Position of Volcanic Flows (after Balkwill, 1978)

CHAPTER 2

ANALYSIS OF DYKE SWARMS OF THE SVERDRUP BASIN

CHAPTER 2

ANALYSIS OF DYKE SWARMS OF THE SVERDRUP BASIN

2.1 Methodology

Figure 1 shows the location of the Sverdrup Basin within the Arctic Islands. Information was gathered using Geological Survey of Canada maps. A list of maps used is found in Appendix I. The map area in Figure 1 was divided up into approximately 200 quadrants, each quadrant being 2 degrees longitude and 1/2 degree latitude in size. The percentage of bedrock showing in each quadrant was estimated (i.e. that area not covered by ice, Quarternary deposits, or water) and recorded.

For each dyke on the map sheets, the following were measured by the author:

- length
- azimuth
- spacing between dykes
- age of the stratigraphic units intruded by the dyke
- fault terminations
- splitting direction of the dyke (if it splits)

A total of approximately 1,600 dykes were measured from the maps. Of the 200 quadrants, approximately 60 contained dykes and all of

these quadrants fell within the limits of the Sverdrup Basin (Figure 1). Stratigraphic units were chosen to coincide with the system used on the maps (eg. Lower Cambrian, Middle Cambrian, Upper Cambrian, Lower Ordovician, etc.)

Rose diagrams with 10 degree intervals were used to plot the dyke orientations since no information on the dip of the dykes is available. Most of the dykes are presumably vertical or nearly vertical.

The database was analysed using an IBM Compaq personal computer. The program used to assist the analyses of the database was dBase III.

Dyke length and spacing was recorded to the nearest millimetre off the maps and the error for these measurements is plus or minus 1/2 mm. converting this to the scale used on the maps gives an actual error of plus or minus 125 m. Error on the azimuth measurement is plus or minus 1 degree.

2.2 Observations

Figure 3a shows dyke frequency contours in number of dykes/100 km^2. Several areas in the map region have very high dyke frequencies. Most notably: Cape Bourne (18.3 dykes/100 km^2), Flat Sound (11.0 dykes/100 km^2), Cape Stallworthy (9.2 dykes/100 km^2), Western Axel Heiberg Island (6.3 dykes/100 km^2), Southern Axel Heiberg (5.9 dykes/100 km^2), and Cornwall Island (5.7 dykes/100 km^2).

Fig 3a: Dyke frequency within the Sverdrup Basin. Contour interval in Dykes/100 km^2 (reference 1)
Fig 3b: Outline of Sverdrup Basin showing axis of basin. (after Ricketts et al., 1985)

Several distinct trends can be discerned on the frequency map. A trend of high frequencies occurs along the northeastern margin of Axel Heiberg Island and another along the southwest margin. A trend of minimum frequencies runs through the central region of the island. All three trends run in a northwest-southeast direction and are roughly parallel to each other. A second, less noticeable trend runs perpendicular to the above trends. A maximum can be seen along the northwest coast of Ellesmere Island with a second maximum running through the central region of Axel Heiberg and Ellesmere island. This second maximum closely parallels the axis of the basin (Figure 3b).

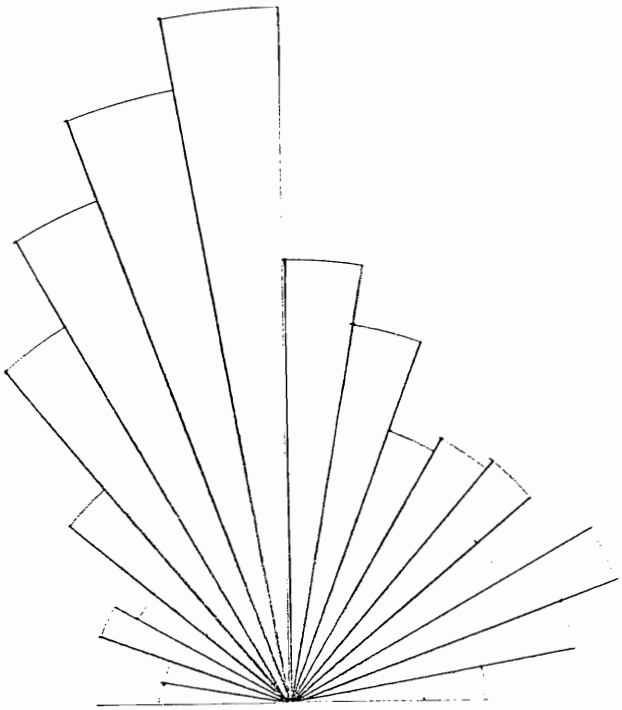

Figure 4 Frequency Rose for Azimuth Trends of Entire Sverdrup Basin. (1,600 dykes)

The frequency rose for azimuth trends of all the dykes combined is shown in Figure 4. Several trends can be seen in the diagram. The strongest trend lies between 350 degrees and 360 degrees but is very broad, extending over a 60 degree interval, from 320 degrees to 020 degrees. Slightly weaker trends are visible from 020 degrees to 050 degrees and 060 degrees to 080 degrees.

Table 1 shows the number of dykes in each of the stratigraphic units, the average length of dykes in each unit, and the average spacing between dykes in each unit.

TABLE 1

Dykes*
Based on Stratigraphic Position

STRATIGRAPHIC HORIZON	NUMBER OF DYKES	AVERAGE LENGTH (m)**	AVERAGE SPACING BETWEEN DYKES (m)**
Lower Cretaceous	344	2,600	1,600
Upper Jurassic	244	2,500	1,500
Middle Jurassic	100	2,100	1,300
Lower Jurassic	138	2,200	1,100
Upper Triassic	592	2,100	1,100
Middle Triassic	223	2,200	900
Lower Triassic	240	2,200	1,100
Upper Permian	8	3,300	2,000
Middle Permian	0	-	-
Lower Permian	84	1,800	1,700
Upper Carboniferous	106	1,700	1,600
Middle Carboniferous	0	-	-
Lower Carboniferous	0	-	-
Upper Devonian	0	-	-
Middle Devonian	1	1,300	500
Lower Devonian	0	-	-
Upper Silurian	13	1,800	1,700
Middle Silurian	14	1,800	1,600
Lower Silurian	401	1,000	400
Upper Ordovician	418	1,000	400
Middle Ordovician	17	1,100	800
Lower Ordovician	29	900	1,300
Upper Cambrian	12	1,000	2,100
Middle Cambrian	12	800	1,800

* NOTE: A dyke can occur in more than one stratigraphic unit. For example, if a formation has been dated as Triassic, then each dyke that cuts that formation would be counted in the Lower, Middle and Upper Triassic. This was done only for grouping purposes and in no way affects the results of this paper.

**The distances have been rounded to the nearest 100 metre.

The youngest stratigraphic intervals cut by dykes is the Lower Cretaceous Christopher Formation. From Table 1, there is a rough correlation between dyke length and stratigraphic interval. The longer dykes occur in the younger stratigraphic intervals while deeper in the stratigraphic section they appear to become shorter.

The older strata in the basin consists mostly of carbonate material as opposed to the more clastic material of the younger strata but this seems unlikely to cause the observed correlation. A more probable suggestion is that the dykes "fan out" as they make their way towards the surface. Figure 5 is a graphical representation of the number of dykes in each of the stratigraphic units. From these, one can see that there is a noticeable lack of dykes in some of the stratigraphic intervals. These intervals include: pre-Middle Cambrian; post Lower Devonian to Middle Carboniferous; Middle and Upper Permian; Lower Cretaceous; and to a lesser extent, Middle Jurassic. This is due to the lack of exposure of these intervals because of periods of non-deposition (Figure 2). They can be used to divide the dykes into four groups based on stratigraphic position: Lower Paleozoic - which includes Upper Cambrian to Upper Silurian; Paleozoic - which includes Upper Carboniferous to Lower Permian; Lower Mesozoic - includes Lower to Upper Triassic; and Upper Mesozoic - which includes Lower Jurassic to Lower Cretaceous. This last group is subdivided again into Lower-Middle Jurassic and Upper Jurassic-Lower Cretaceous, mainly

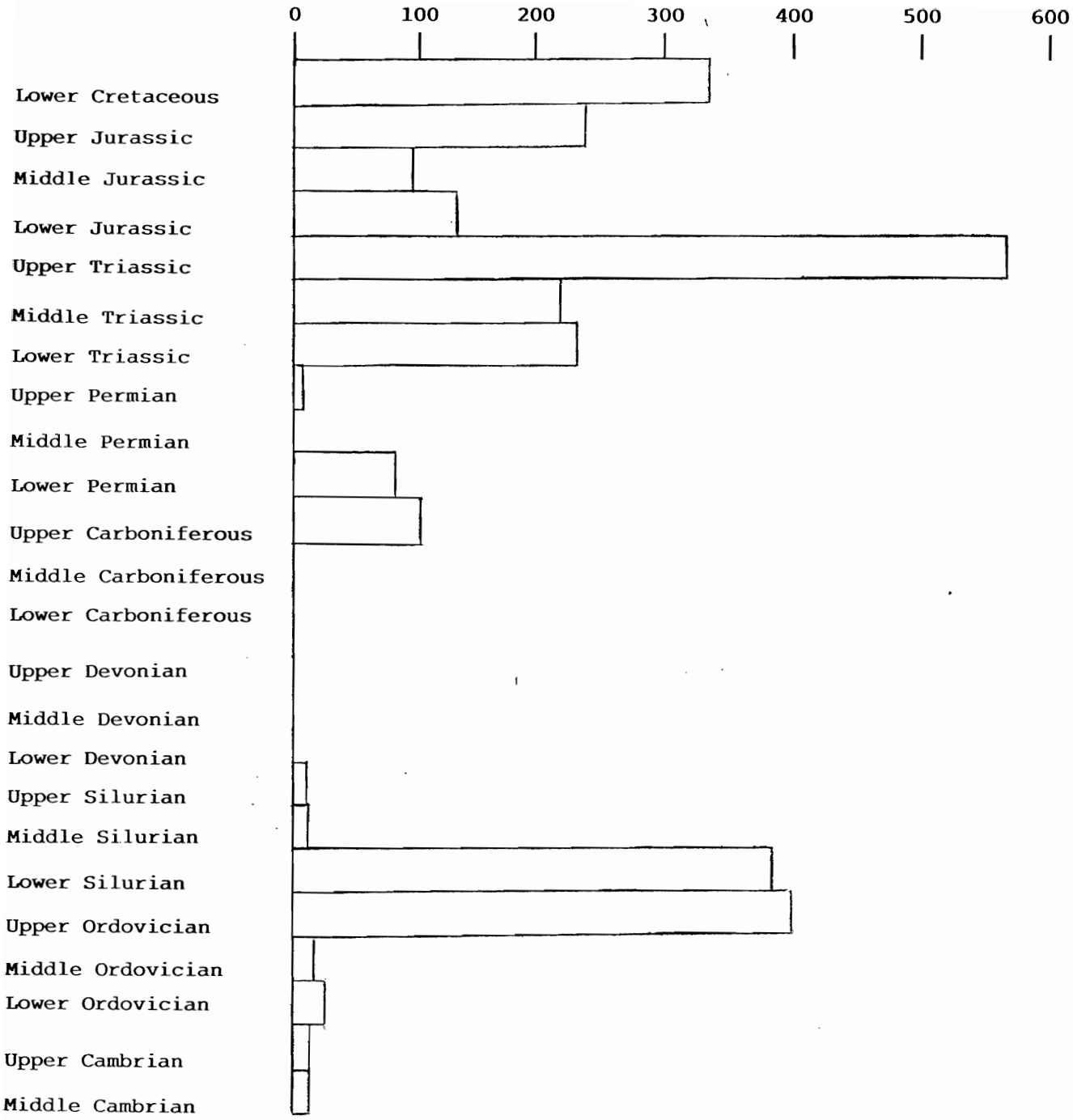

Figure 5: Dyke Frequency in each Stratigraphic Interval

because the average length and distances between the dykes are quite different (see Table 1).

Azimuth frequency roses for each of the five groups show distinct differences between the groups. The Upper Jurassic to Lower Cretaceous group shows strong preferential directions between 030 degrees - 050 degrees; and 060 degrees - 080 degrees with some overlap between the two (Figure 6). The Lower to Middle Jurassic group has several strong tendencies from 000 degrees - 020 degrees; 040 degrees - 050 degrees; 060 degrees - 070 degrees; and 320 degrees - 350 degrees (Figure 7).

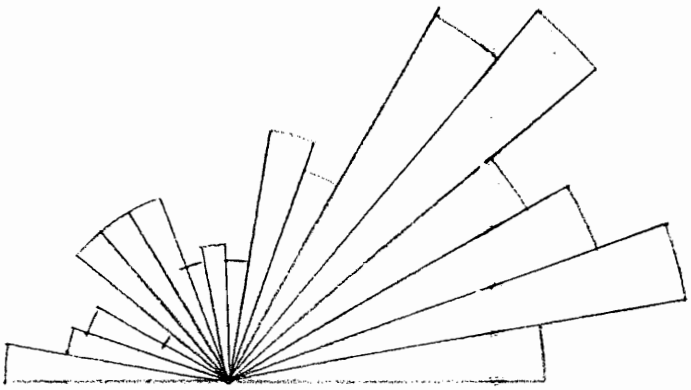

Figure 6: Frequency Rose for Upper Jurassic and Lower Cretaceous (298 dykes)

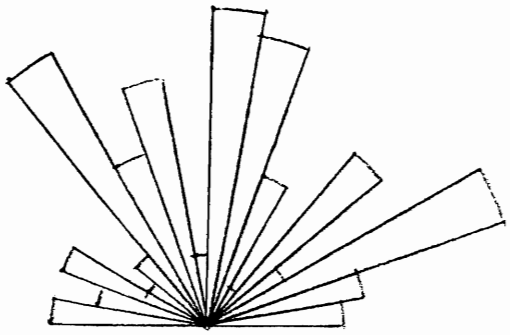

Figure 7: Frequency Rose for Lower and Middle Jurassic (139 dykes)

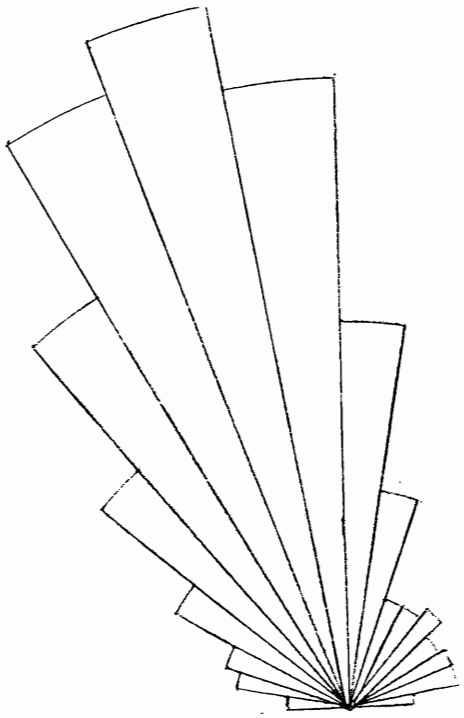

Figure 8: Frequency Rose for Lower Mezozoic (621 dykes)

The Lower Mesozoic group has a very broad, powerful trend from 320 degrees to 010 degrees peaking between 340 degrees and 350 degrees (Figure 8). The Upper Paleozoic group shows preferred directions between 350 degrees - 360 degrees; and 010 degrees - 020 degrees (Figure 9). The last group, which includes Lower Paleozoic strata, has a very strong sharp trend between 350 degrees and 360 degrees with weaker trends from 020 degrees - 040 degrees and 060 degrees - 070 degrees (Figure 10).

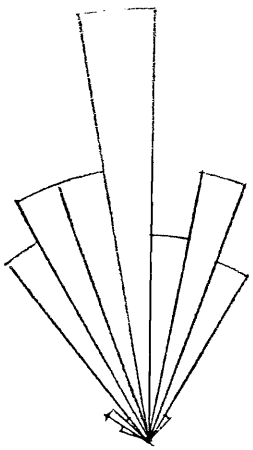

Figure 9: Frequency Rose for
Upper Paleozoic
(84 dykes)

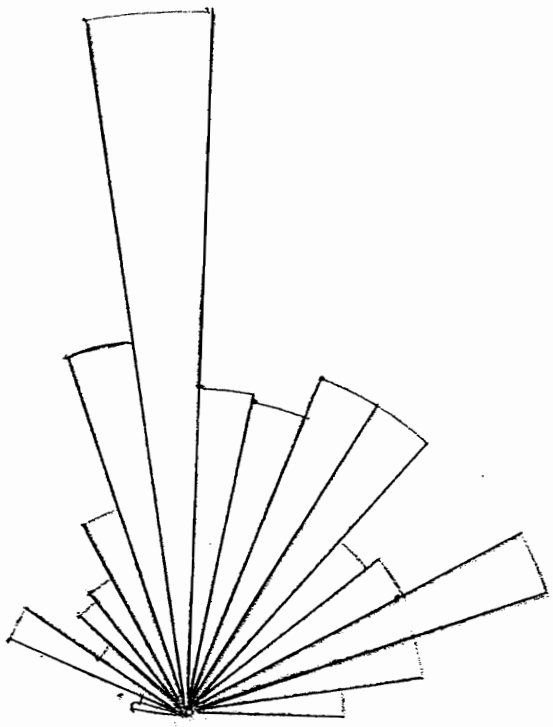

Figure 10: Frequency Rose for Lower Paleozoic (449 dykes)

Table 2 summarizes differences of dykes within each of the preferred directions for all five groups.

TABLE 2

Differences Between
Trends Within Groups

GROUP	TREND	COUNT	AVERAGE LENGTH (m)	AVERAGE SPACING (m)	LENGTH/ SPACING	FAULT TERMINATIONS	SPLITS
Upper Jurassic - Lower Cretaceous	A (030-050)*	60	2,700	1,700	1.41	6	3
	B (060-080)*	57	2,800	1,300	2.15	5	5
	C (310-340)	39	2,200	1,100	2.00	2	5
	D (000-020)	25	2,500	3,400	0.73	3	1
Lower - Middle Jurassic	B (060-070)*	14	2,500	1,700	1.46	0	4
	D (000-020)*	27	2,400	1,100	2.18	0	5
	C (320-350)	33	2,100	1,100	1.18	5	2
	A (040-050)	10	1,800	1,600	1.12	1	0
Lower Mesozoic	C (320-360)*	329	2,100	1,300	1.61	27	11
	D (000-020)	81	2,500	1,100	2.27	5	6
	A & B (040-080)	61	1,800	600	3.00	4	5
Upper Paleozoic	C (350-360)*	19	1,700	900	1.88	4	0
	D (010-020)	12	1,400	1,200	1.16	4	0
Lower Paleozoic	C (350-360)*	69	1,000	400	2.50	2	2
	B (060-070)	37	800	500	1.60	0	1
	A (020-040)	70	1,000	400	2.50	0	4
	D (000-020)	63	1,000	300	3.33	1	2

* Dominant Trends

The preferred orientation of the dykes changes within the Sverdrup Basin. The strong northerly trend is most pronounced along the western margin of Ellesmere Island and in northern and eastern Axel Heiberg Island. Moving west the trend gradually swings into a more easterly direction. Figure 11 shows this nicely. The most prominent trend is in red, while the second

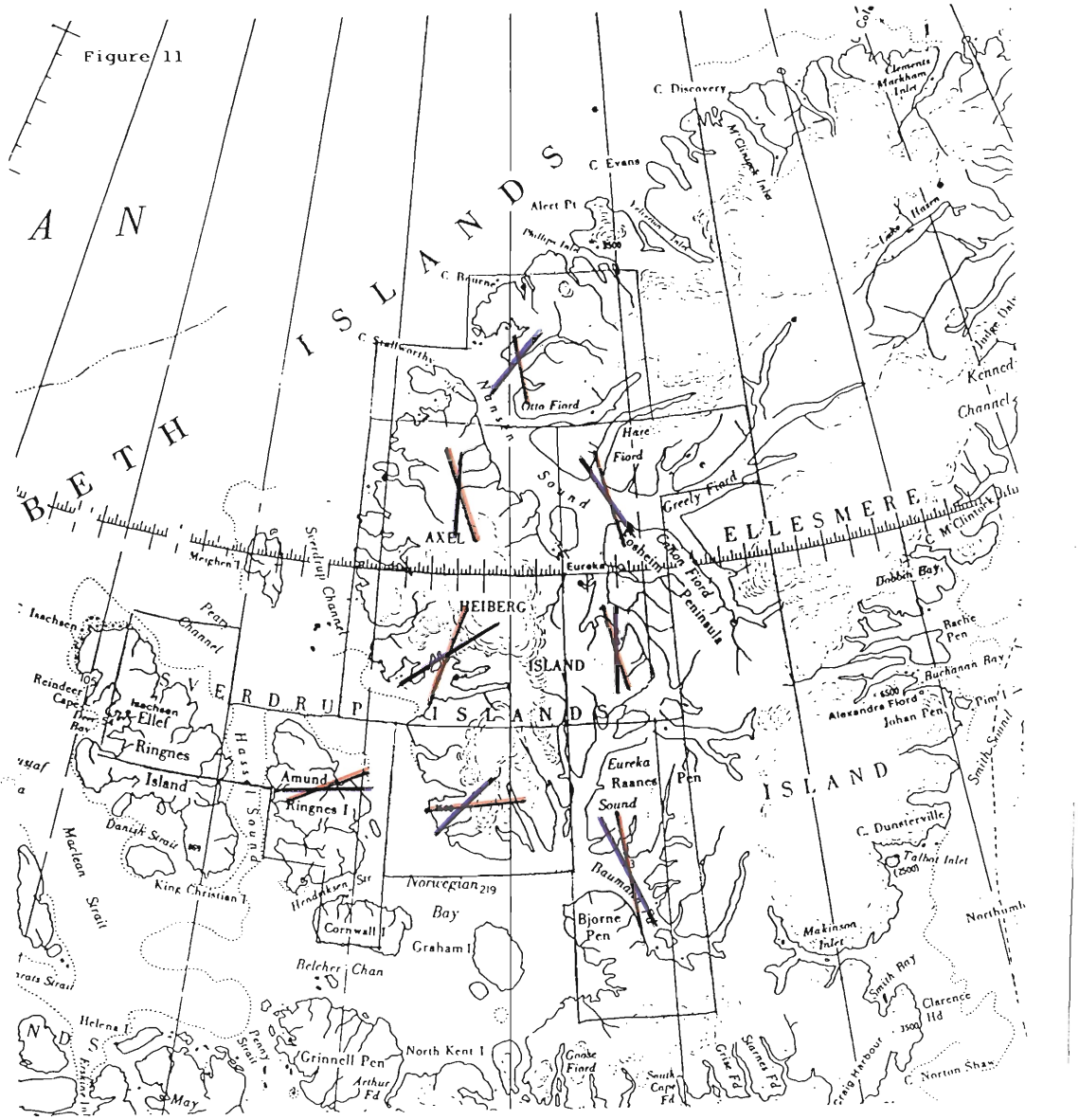

most prominent is in blue. This distribution also reflects the bedrock distribution of the Sverdrup Basin. The northerly trends are found along the western margin of the Sverdrup Basin and consist mostly of Triassic and Paleozoic rocks. The easterly trends are found more towards the center of the basin where Cretaceous and Upper Jurassic rocks are located (Figure 12).

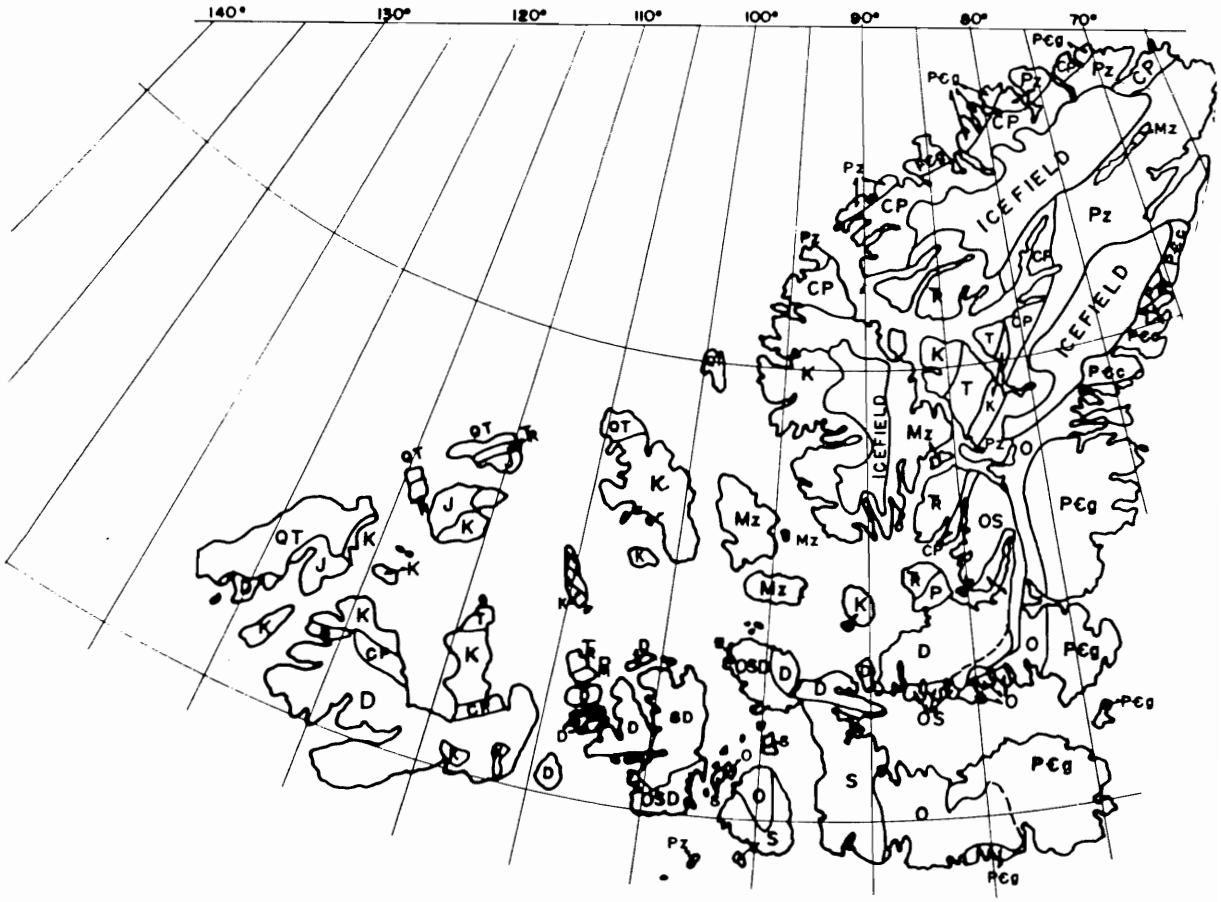

Figure 12: Bedrock Geology Map of the Arctic Region (reference 10)

QT - Quaternary	D - Devonian
T - Tertiary	O - Ordovician
K - Cretaceous	S - Silurian
Tr - Triassic	Mz - Mesozoic
CP - Carboniferous - Permian	Pz - Paleozoic
PCg - Precambrian	

2.3 Analysis

From Table 2, several distinct swarms can be observed. These swarms differ from each other mainly on the basis of azimuth. They also differ slightly on the basis of length, spacing, fault terminations and number of splits within each of the stratigraphic groups (since the dykes tend to be shorter within the older groups, the younger groups cannot be directly compared with the older groups).

Swarm A includes:

030-050 Upper Jurassic and Lower Cretaceous
040-040 Lower and Middle Jurassic
040-050 Lower Mesozoic
020-040 Lower Paleozoic

Swarm A is not observed in the Upper Paleozoic group, probably because the number of dykes within this group is rather small, and the results are not as meaningful as the other, larger groups. Swarm A is the dominant swarm in the Upper Jurassic and Lower Cretaceous group.

Swarm B includes:

060-080 Upper Jurassic and Lower Cretaceous

060-070 Lower and Middle Jurassic

060-080 Lower Mesozoic

060-070 Lower Paleozoic

Swarm B is not present in the Upper Paleozoic for the same reasons Swarm A is not. Swarm B is also dominant in the Upper Jurassic and Lower Cretaceous group.

Swarm C includes:

310-340 Upper Jurassic and Lower Cretaceous

320-350 Lower and Middle Jurassic

320-360 Lower Mesozoic

350-360 Upper Paleozoic

350-360 Lower Paleozoic

This swarm dominates in the Lower Mesozoic and older sediments.

Swarm D includes:

010-020 Upper Jurassic and Lower Cretaceous

000-020 Lower and Middle Jurassic

000-020 Lower Mesozoic

010-020 Upper Paleozoic

000-020 Lower Paleozoic

Swarm D is present in all groups but is not dominant in any one of them.

The distribution of these stratigraphic groups is not uniform throughout the basin. Triassic and older rocks are found along the northern margin of the basin while younger sediments occur more southward toward the middle of the basin (Figure 12). This is reflected in Figure 11 which shows prominent trends in various areas of the basin.

This distribution is also reflected in Figure 3a, which has a prominent northwest trend of maximum dyke frequencies near the northern margin of the basin and a northeast trend in younger rocks towards the center of the basin.

2.4 Interpretation

All four swarms are found in each of the stratigraphic groups, except in the Upper Paleozoic where it is felt that the numbers are too small to accurately reflect the swarm distribution. This suggests that all of the swarms are of nearly the same age. However, in the youngest stratigraphic group, Swarms A and B dominate while in the Lower Mesozoic and older groups, Swarm C dominates. The Lower and Middle Jurassic group represents a transition area between Swarm C dominating in the older sediments and Swarms A and B dominating in the Upper Jurassic and Lower Cretaceous group.

Based on the data that has been collected, the major dyking episodes probably all occurred during the Cretaceous. All trends can be observed in rocks up to that age. However, until adequate absolute age dating of the dykes is available, one cannot exclude the possibility that some of the trends may have originated during earlier (i.e. Permian) igneous episodes, and were reactivated during the Cretaceous.

The author believes that there has been two major dyking episodes during the Cretaceous. The first dyking event was dominated by Swarm A and Swarm B trends. This dyking has occurred throughout the Sverdrup Basin and the dominant trends lie sub-parallel to the axis of the basin. This leads to the possibility that dyking trends were controlled by structural trends that were developed during the extension and subsidence of the basin. A second event, also in the Cretaceous, occurred either before, during or after the emplacement of the first set of dykes. These dykes belong to Swarms C and D. They were concentrated more towards the northern end of the basin and occurred in a wide swath roughly in line with, and parallel to, the Alpha Ridge complex.

A maximum in dyke frequency (Figure 3a) occurs in norther Axel Heiberg and northwestern Ellesmere Island. Recent field investigations has shown that substantial thicknesses of Cretaceous extrusive volcanics are present in this area (K. Osadetz, ISPG, pers. comm.). Also, dykes in the region show Cretaceous paleopoles. The high dyke frequency, alignment of

trends with the Alpha Ridge, (Figure 1b) presence of major amounts of extrusive volcanics, and proximity to the continental margin suggest that the volcanic activity in this region represents that landward continuation of the Alpha Ridge complex. These dykes did not intrude the more central parts of the basin where the sediments are younger and as a result, the north trending C and D Swarms are not as pronounced in the younger stratigraphic groups.

An alternate, but less attractive interpretation is that the dyking follows the outline of the basin. This is true for the northeast and east trending A and B Swarms. They generally tend to follow the basin outline, but the C and D Swarms cut directly across it in the vicinity of Nansen Sound (Figure 1).

CHAPTER 3

LIGHTFOOT RIVER DYKES

CHAPTER 3

LIGHTFOOT RIVER DYKES

3.1 Introduction

The Lightfoot River area, central Axel Heiberg Island, was chosen for a petrographic and geochemical study mainly because the dykes in this area are contained within the prominent north-northwest trending swarm. Samples were collected by Marie-Claude Williamson during the 1985 field season.

3.2 Setting

Ten dykes were sampled in the Lightfoot River area (Figure 13 and 14). Thicknesses of the dykes ranged from 1 metre up to 60 metres. Samples were taken from various positions within each dyke (see Appendix II). The dykes that were sampled all intrude sediments of the Triassic Blaa Mountain Formation or of the Lower Triassic Blind Fiord Formation. The only other formation intruded by the dykes in this area is the Upper Carboniferous - Lower Permian Nansen Formation. The rocks that have been intruded consist mainly of shales, siltstones and sandstones.

Figure 13: Study Locations on Axel Heiberg Island (after Williamson, 1985)

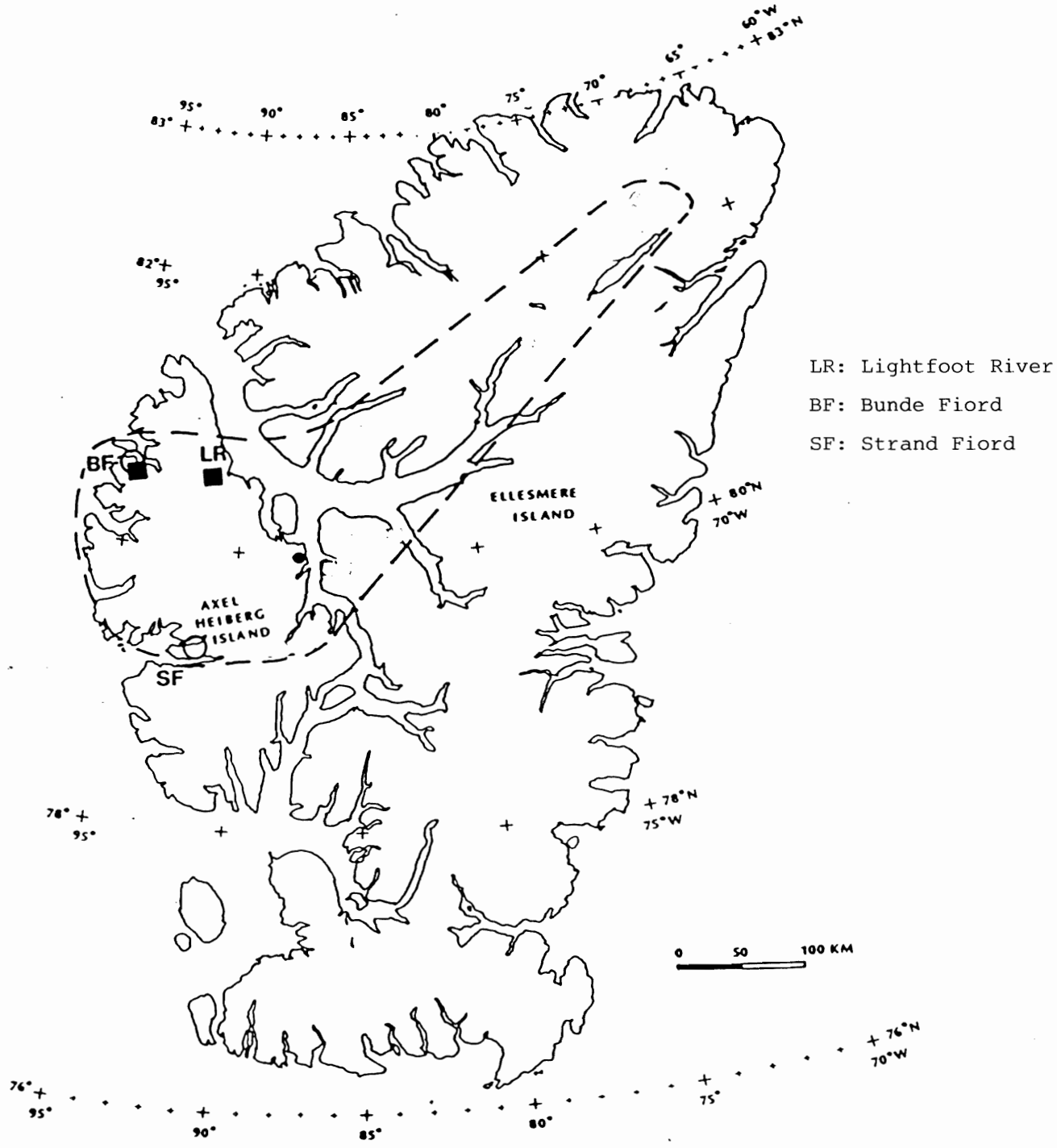

Figure 14: Lightfoot River Area (after Williamson, April, 1985)

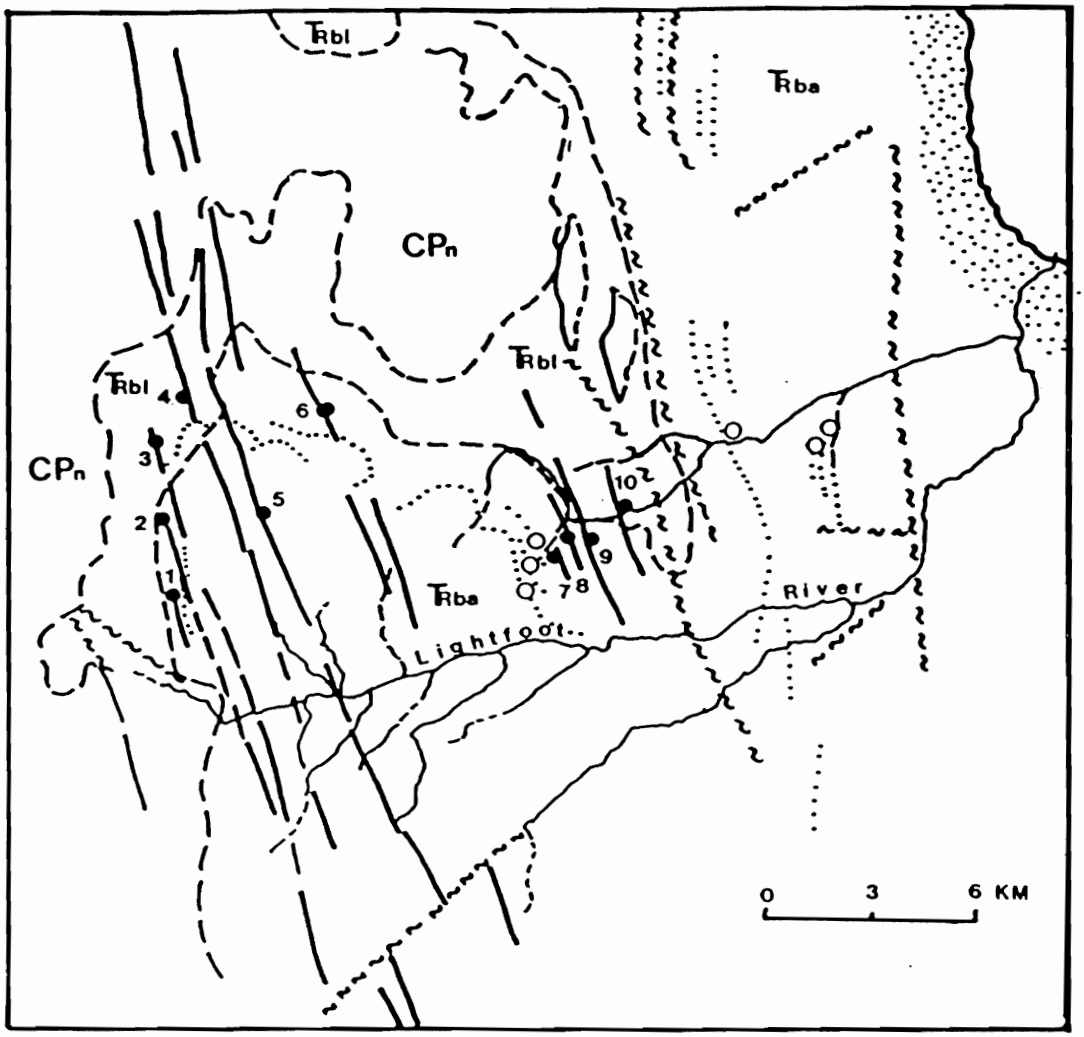

LOWER, MIDDLE AND UPPER TRIASSIC

TRba — BLAA MOUNTAIN FORMATION: dark coloured shale and siltstone ★

LOWER TRIASSIC

TRbl — BLIND FIORD FORMATION: siltstone; minor shale and sandstone

UPPER CARBONIFEROUS AND LOWER PERMIAN

CPn — NANSEN FORMATION: limestone, chert; minor shale and siltstone

★ light grey calcareous siltstone, minor sandstone

SILL — O sampled

1 DYKE — ● sampled

FAULT

GEOLOGICAL BOUNDARY

3.3 Petrography

3.3.1 Hand Samples

The only hand sample available for examination is the chilled margin of Dyke #2. This sample is very fine-grained with grain sizes estimated in the order of Ø.1 mm to Ø.5 mm. Weathered surfaces show reddish oxidation. Fresh surfaces show small (approximately Ø.5 mm) light colored crystals, probably feldspar, and even smaller (approximately Ø.1 mm) black crystals set in a dark grey matrix. No other minerals can be readily identified due to the small grain size.

3.3.2 Thin Sections

All ten of the dykes examined were mineralogically similar, although texturally they were different depending on their position within the dyke. The dykes have very fine grained chilled margins, commonly with intersertal or porphyritic textures. Occasionally textures are hyalopilitic or felty (Plate 2b). More towards the middle of the dykes, the grain size is much coarser, especially in the thicker dykes, where crystals can be up to 5 mm long. Textures also change more towards intergranular which reflects the slower cooling rate (Plate 3a). Ophitic and subophitic textures are also very common.

Plagioclase is the most abundant mineral in the sections, making up from 40-65 percent of the rock. It occurs mainly as large euhedral to subhedral crystals, (Plate 3b) and probably is one of the first crystallizing phases in the rock. Michel-Levy determinations suggest that compositions range from andesine to labradorite with most tending towards andesine. Alteration of the plagioclases is severe, often to the extent that plagioclase is entirely sericitized.

Clinopyroxenes generally make up from 5 to 30 percent of the samples. They occur as anhedral crystals, (Plate 3b) generally smaller than plagioclase laths. Clinopyroxene is commonly pale green in thin section. Some of the clinopyroxene is retrogressively altered to tremolite (Plate 4a) while the rest shows some reddish alteration.

Oxides, probably magnetite, are quite common in the samples, comprising up to 15 percent. Often these are present as euhedral crystals, octahedral and sometimes triangular in thin section. They also showed some reddish alteration. Some sections showed severe corrosion.

Accessory minerals include biotite, quartz, apatite, ilmenite, and calcite. Biotite has been altered to chlorite in most cases. Quartz is always present in the thin sections, interstitial between larger grains of plagioclase and clinopyroxene. Ilmenite occurs as long narrow, needle-like crystals arranged in parallel groups (Plate 4b). Calcite is a replacement mineral that occurs in most samples. It

appears to replace clinopyroxene most often but is also observed to replace quartz and plagioclase. No olivine was observed in any of the sections. A more detailed description of the mineralogy can be found in Appendix III.

CHAPTER 4

GEOCHEMISTRY

CHAPTER 4

GEOCHEMISTRY

4.1 Methodology

Ten samples from the Lightfoot River area (Figure 14) were analysed for major and trace element composition. Each rock sample weighed approximately 50 g. The sample was broken into small fragments using a hydraulic press and a ceramic jaw crusher. These small chips were ground in a tungsten carbide container secured to a swing mill. Approximately 30 g of powder was homogenized by hand and sieved to 80 mesh. For the major element analysis, exactly 1 g of this powder is combined with 5 g of lithium tetraborate and fused into a glass disk and analysed. For the trace elements, approximately 9 g plus binder are made into a compressed pellet, baked, then analysed.

The samples were analysed at the X-Ray Florescent Facility, Saint Mary's University (Kevin Cameron, analyst) using a Philips TW1400 XRF Machine.

CIPW norms have been calculated using corrections by Irvine and Baragar (1971). Because iron is reported as Fe_2O_3 in the analysis, an accurate CIPW norm is impossible unless some is converted to FeO. Irvine and Baragar (1971) argue that maximum amount of Fe_2O_3 in unaltered volcanics is equivalent to:

$$\% Fe_2O_3 = \% TiO_2 + 1.5 \quad (1)$$

Fe_2O_3 in excess of this value is converted to FeO using equation (2).

$$\% Fe_2O_3 \times Ø.8998 = \% FeO \quad (2)$$

The results of the analyses are shown in Table 3. CIPW norms are shown in Table 4.

4.2 Dyke Geochemistry and Variation

In conformity with the petrographic observations, all the samples are basaltic in composition. Their SiO_2 range from 46.46 to 51.89 etc. On an AFM diagram the dykes follow the tholeiitic trend rather than that of calk-alkaline rocks (Figure 15).

In the CIPW Basalt tetrahedron the rocks fall well within the quartz normative tholeiites (Figure 16). This is confirmed by the modal composition of the rocks observed under thin section. The rocks also have average potassium values for sub-alkaline rocks (Figure 17) based on the An - Ab' - Or diagram developed by Irvine and Baragar (1971).

TABLE 3

SAMPLE	AX85-15	AX85-19	AX85-20	AX85-26	AX85-31
SiO_2	51.89	49.86	48.53	49.64	49.29
TiO_2	2.28	2.75	3.29	3.65	3.67
Al_2O_3	13.34	13.40	12.99	12.44	14.92
Fe_2O_3	12.89	14.78	15.43	14.93	13.23
MnO	0.18	0.25	0.23	0.18	0.17
MgO	5.03	4.11	4.89	5.21	4.87
CaO	8.90	7.37	8.15	8.32	7.93
Na_2O	2.74	3.53	3.23	3.13	3.11
K_2O	1.07	1.13	1.11	0.79	1.45
P_2O_5	0.28	0.58	0.40	0.44	0.33
LOI*	1.70	1.40	1.90	1.60	1.40
TOTAL	100.30	99.16	100.15	100.33	100.37
Ba	277	500	582	141	386
Rb	27	22	32	24	47
Sr	257	313	399	343	469
Y	45	51	39	46	42
Zr	250	276	220	278	227
Nb	25	26	22	21	17
Th	2	5	2	3	0
Pb	14	11	12	9	5
Ga	22	22	21	21	23
Zn	127	288	166	112	88
Cu	60	49	52	124	146
Ni	35	21	22	39	35
V	332	329	444	415	399
Cr	58	8	11	38	62

Majors in weight %

Minors in ppm.

* LOI - Loss on Ignition

TABLE 3
(Continued)

SAMPLE	AX85-35	AX85- 40	AX85-43	AX85-46	AX85-48
SiO_2	47.34	49.42	48.74	51.80	46.46
TiO_2	4.10	3.11	2.76	2.03	3.64
Al_2O_3	12.47	12.06	12.27	12.51	11.94
Fe_2O_3	15.86	15.54	15.94	14.15	17.13
MnO	0.19	0.22	0.23	0.22	0.25
MgO	4.81	4.98	5.02	5.19	6.02
CaO	8.70	8.37	7.80	8.21	6.99
Na_2O	2.78	2.52	3.06	2.86	3.22
K_2O	0.72	1.21	1.19	0.85	0.33
P_2O_5	0.61	0.41	0.33	0.21	0.46
LOI*	1.50	1.40	2.20	1.50	3.40
TOTAL	99.08	99.24	99.54	99.53	99.84
Ba	214	616	572	275	393
Rb	17	36	30	28	9
Sr	353	325	410	299	402
Y	59	51	43	41	42
Zr	319	229	207	195	198
Nb	22	22	22	16	24
Th	4	3	2	0	5
Pb	8	7	9	9	12
Ga	27	21	24	19	22
Zn	68	136	143	127	173
Cu	68	100	57	102	47
Ni	48	31	24	31	23
V	502	460	433	364	515
Cr	44	27	10	33	11

Majors in weight %

Minors in ppm.

* LOI - Loss on Ignition

TABLE 4

CIPW NORMS

	Qtz	or	ab	an	di	hy	mt	il	ap
AX85-15 An=47	7.00	6.32	23.19	20.94	17.45	12.12	5.63	4.52	0.65
AX85-19 An=37	3.90	6.68	29.83	17.38	12.69	13.08	6.41	5.55	1.34
AX85-20 An=39	2.75	6.56	27.33	17.67	16.42	11.80	7.29	6.70	0.93
AX85-26 An=40	6.05	4.67	26.49	17.56	16.80	10.39	7.71	7.26	1.02
AX85-31 An=46	4.19	8.57	26.32	22.47	11.71	9.45	7.64	7.16	0.76
AX85-35 An=45	6.33	4.26	23.52	19.42	15.91	9.26	8.45	8.22	1.41
AX85-40 An=46	6.26	7.15	21.32	18.02	17.06	13.18	6.81	6.08	0.95
AX85-43 An=39	2.75	7.03	25.89	16.23	16.71	14.73	6.60	5.79	0.76
AX85-46 An=44	6.41	5.02	24.20	18.79	16.95	16.00	5.21	3.97	0.49
AX85-48 An=39	2.86	1.95	27.25	17.15	11.82	18.22	7.81	7.39	1.07

Dyke number 9 (21.5 m wide) and dyke number 5 (60 m wide) each had samples collected near their margins and towards the interior. Comparison of these samples provides some information on gross differentiation trends within the dykes, but to rigorously examine such trends a more systematic and thorough

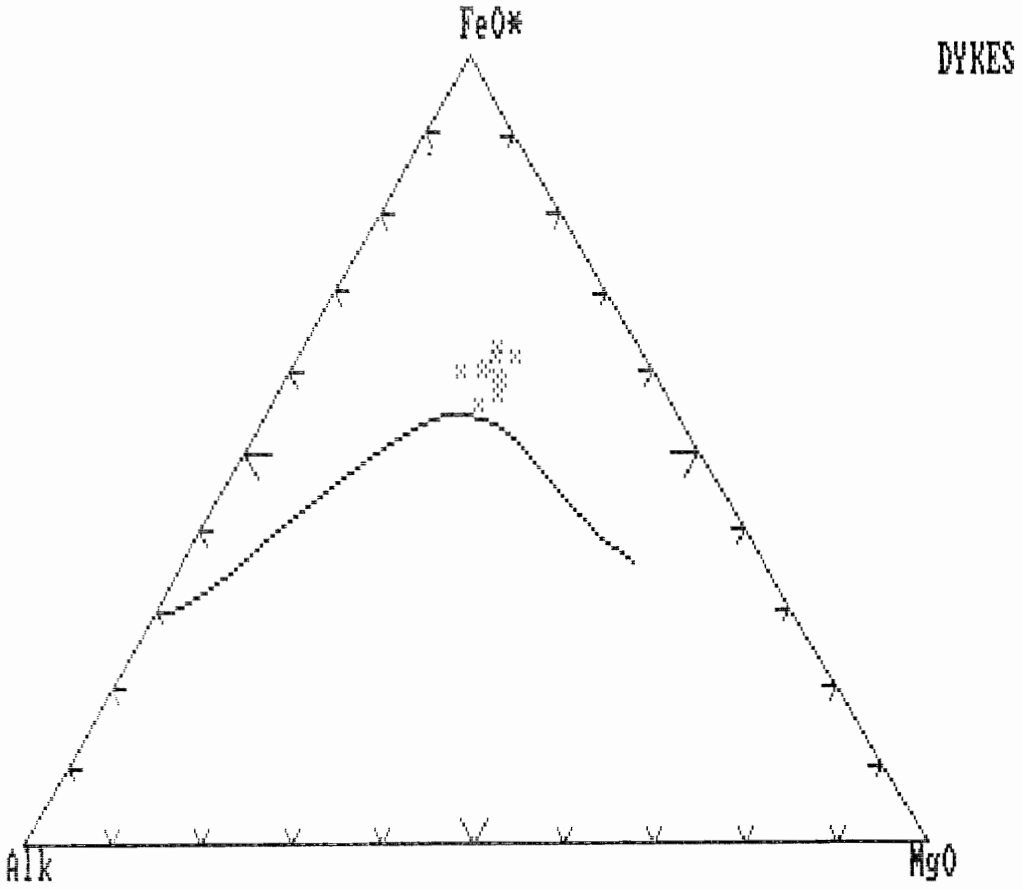

Figure 15

sampling and analyses of the dykes is required. Dyke 9 tends to follow an element distribution pattern that would be predicted if crystal fractionation played a major part during the cooling of the dyke. Such differentiation may occur as the dykes cooled form its margins to the interior or as a result of flow

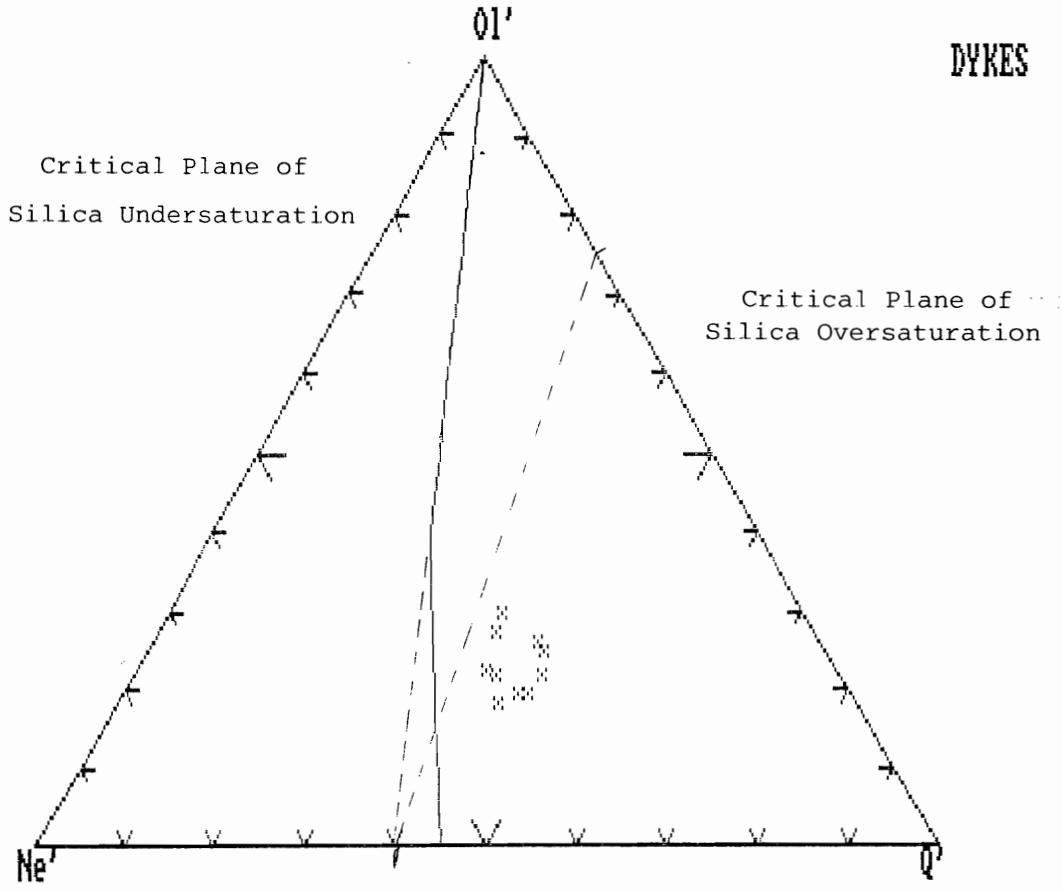

Figure 16

differentiation (Barker, 1983, Best, 1982) Increasing in silica, $Al2O_3$, K_2O, P_2O_5, Y, Zr and Nb towards the interior while decreasing in TiO_2, Fe_2O_3, MgO and CaO observed in dyke 9 conform to early crystallization and extraction of high T-phases such as cpx and calcic plagioclase (Figure 17). Dyke 9 departs from predicted patterns for Ba, Rb and Sr since these are enriched in the margin areas. These elements are geochemically mobile, (Humphris and Thompson, 1978b) and since the country rocks (shales, sandstones, and siltstones) are enriched with these elements relative to tholeiites, it is probable that the margins

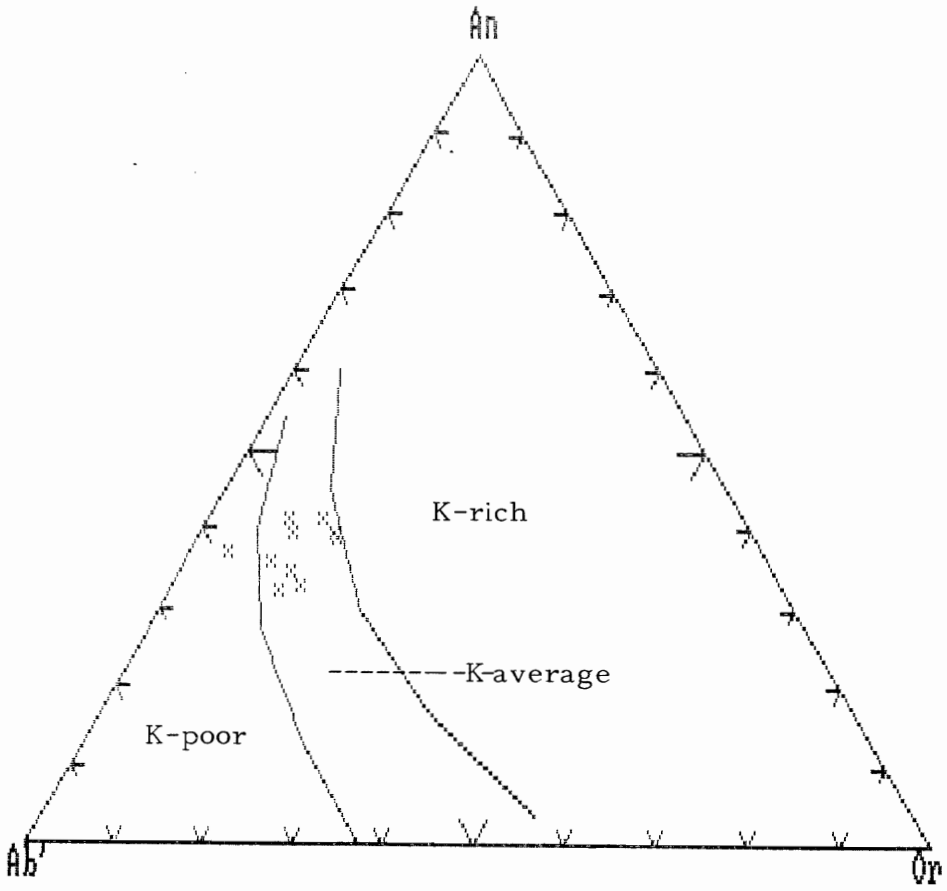

Figure 17

In the following Figures 18 and 19, the major element oxides are recorded as weight percent. Trace elements are recorded in parts per million.

Numbers on the Figures refer to the dyke number (e.g. #5 refers to Dyke 5 on Figure 14).

- Number 11 represents the average value for volcanics in the Bunde Fiord Region.

- Number 12 represents the average value for volcanics in the Strand Fiord Region.

Arrows represent trends from margins of dykes to interiors

Figure 18a

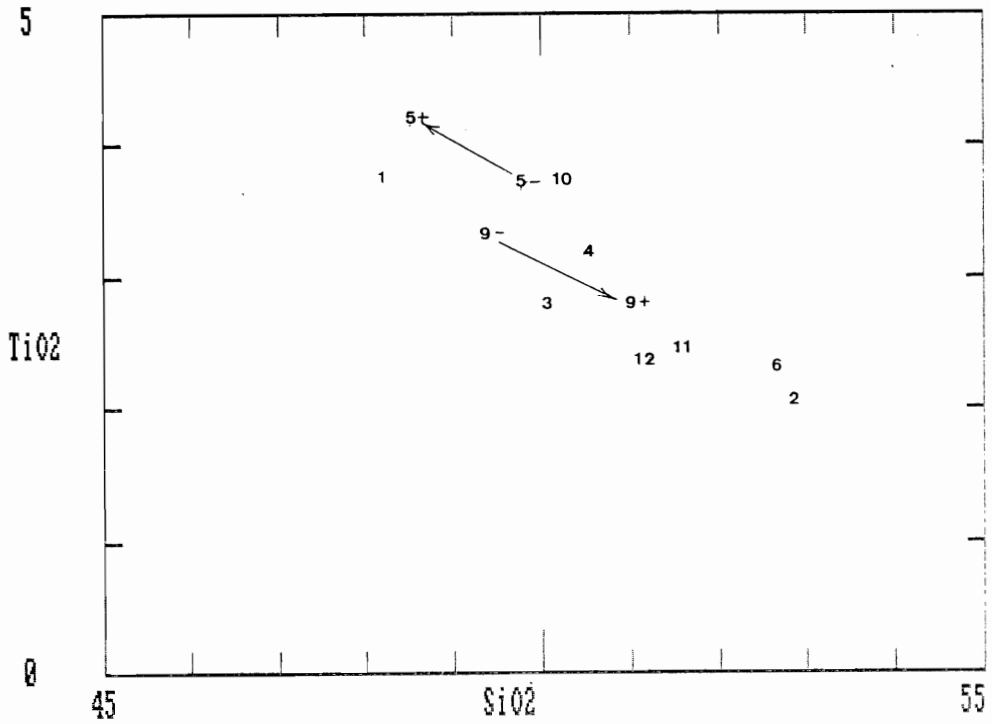

Figure 18b

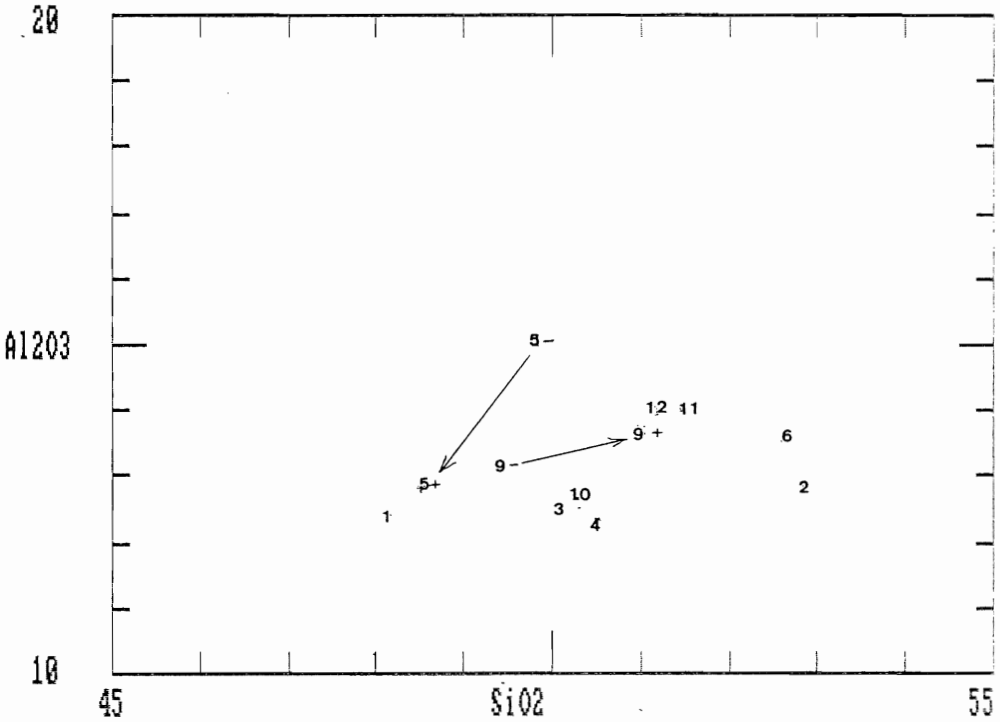

Figure 18c

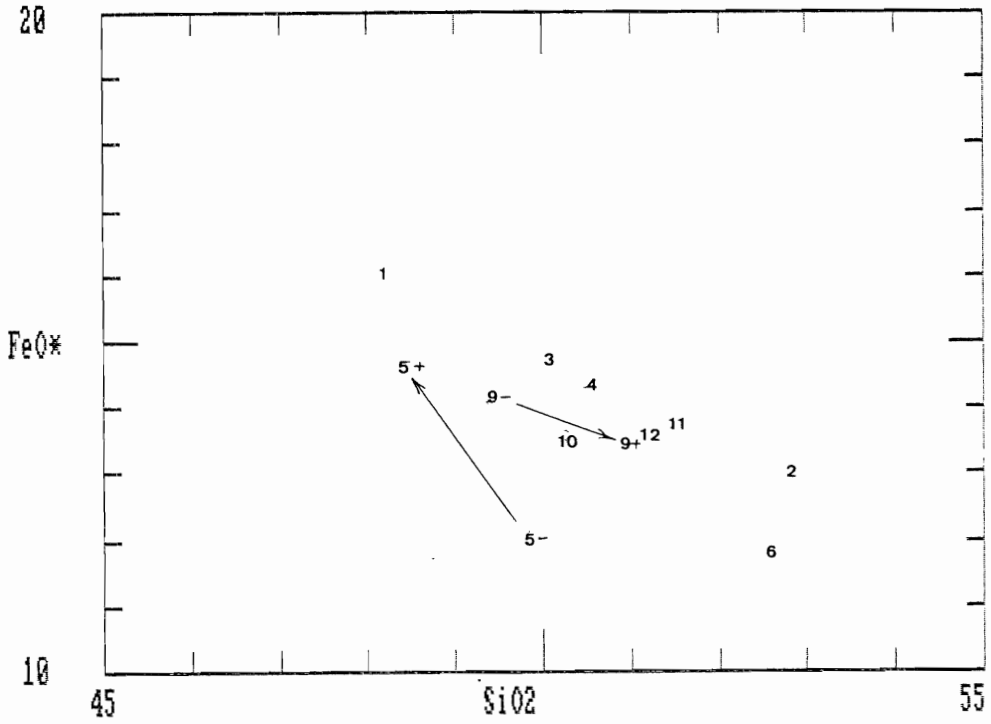

Figure 18d

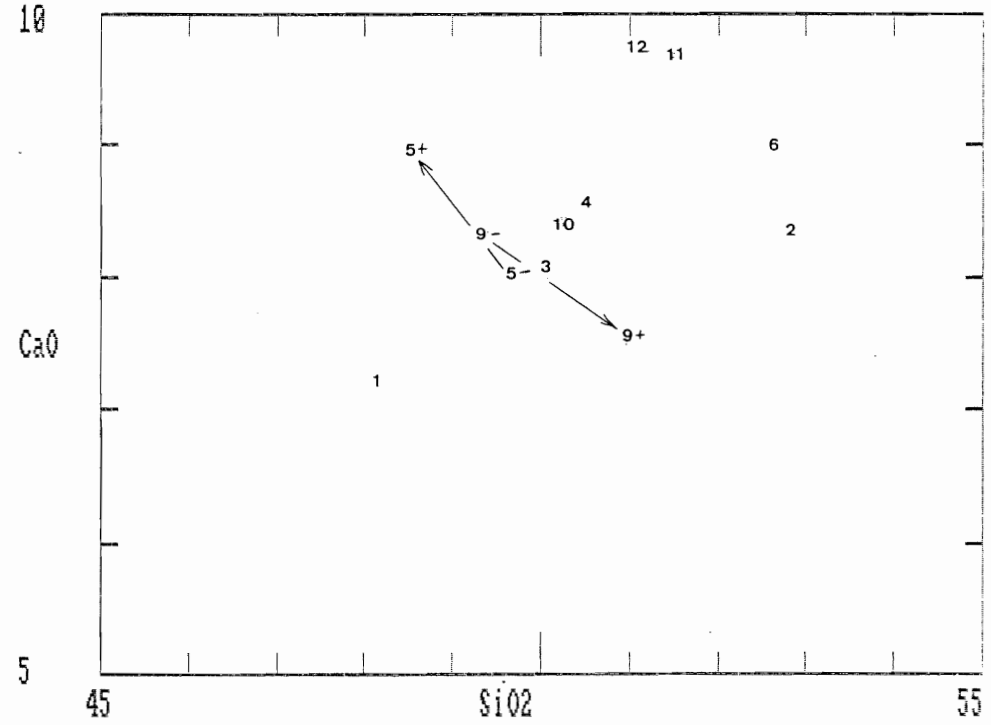

Figure 18e

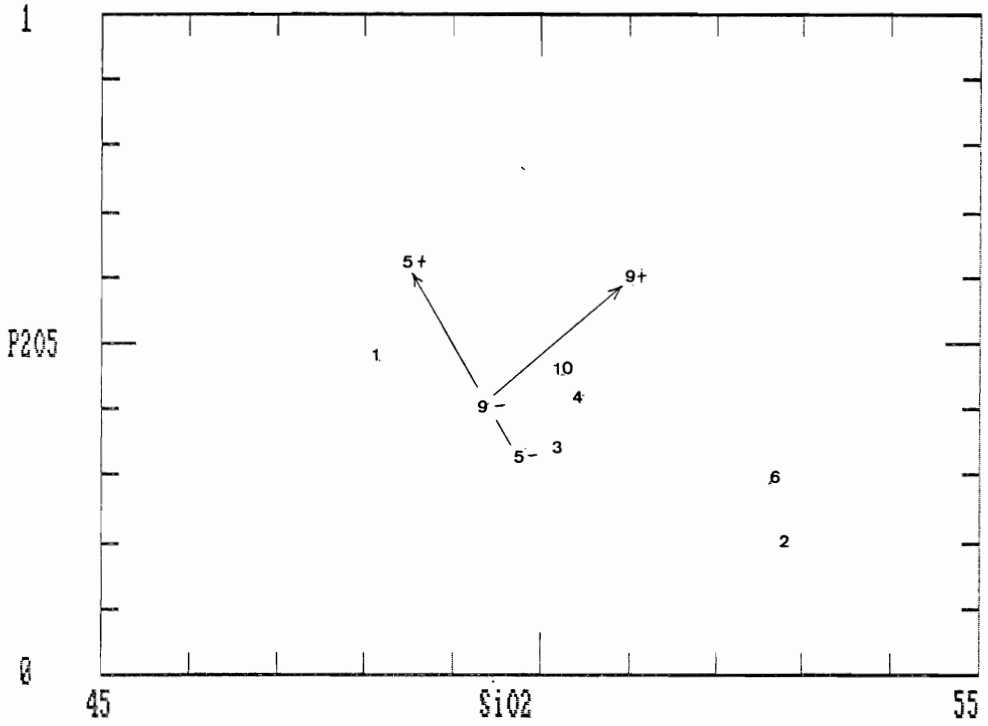

Figure 18f

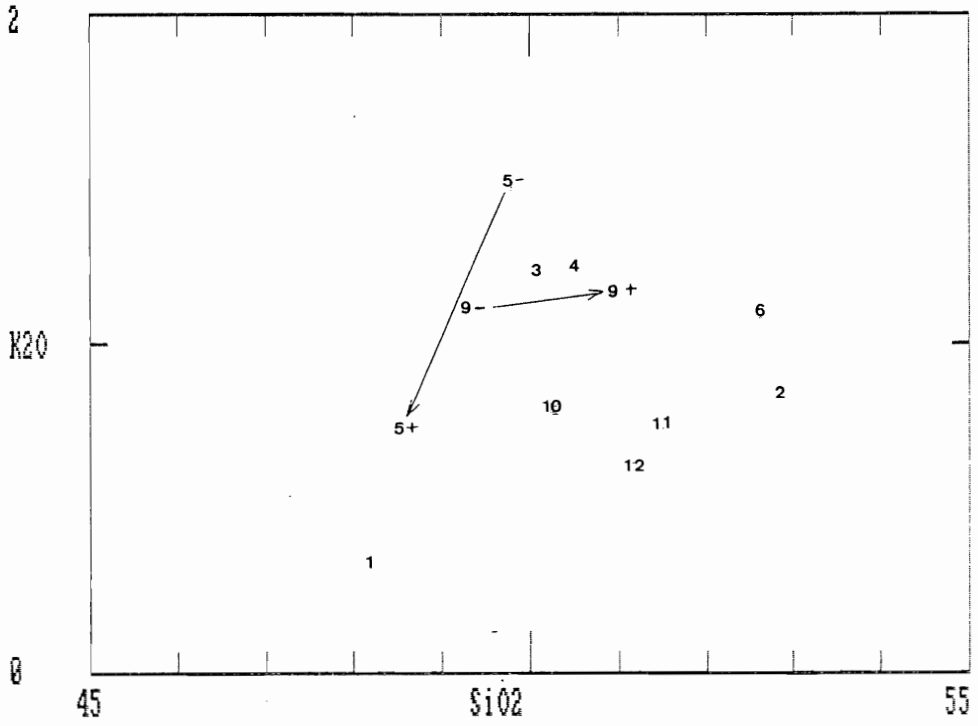

have been contaminated by the country rocks. Dyke 5 also shows this enrichment of Ba, Rb and Sr near the margins but much more strongly (i.e. Ba). However, dyke 5 further departs from predicted patterns with silica, TiO_2, Al_2O_3, Fe_2O_3, MgO and K_2O (Figure 18). These trends run opposite of what might be expected from normal crystal fractionation trends. Wall rock contamination or possibly contamination from xenoliths of country rock may be the reason for the unexpected results. Xenoliths of wall rock were observed in the field. Relatively immobile elements such as Y, Zr and Nb follow the predicted patter for crystal fractionation suggesting that it has occurred (Figure 19) in both of the dykes.

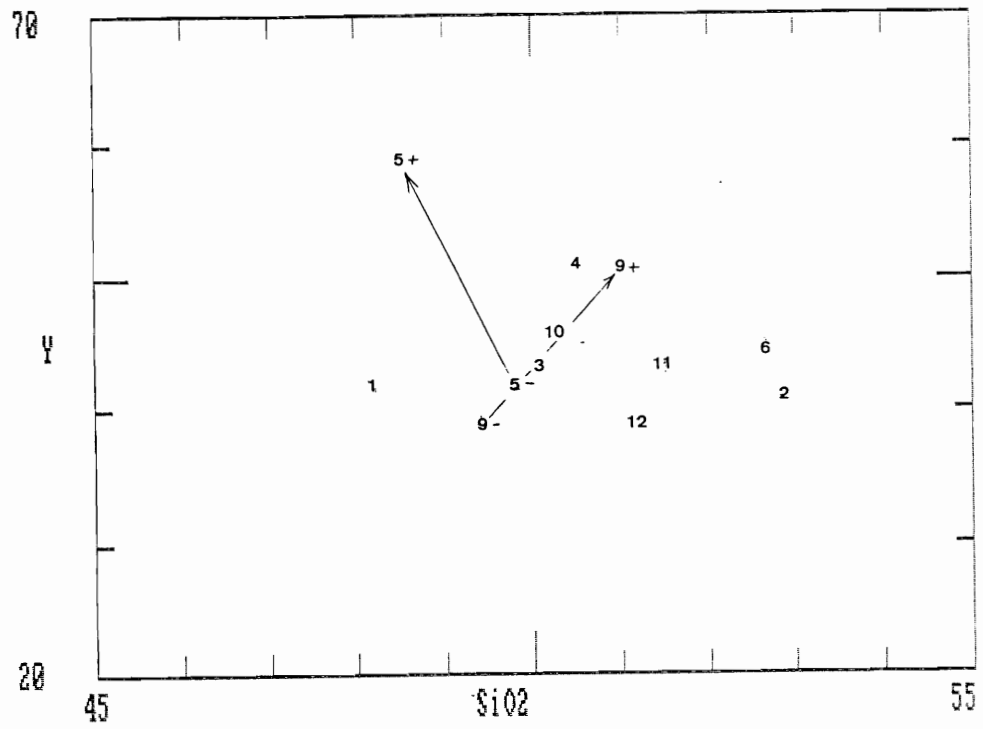

Figure 19a

Figure 19b

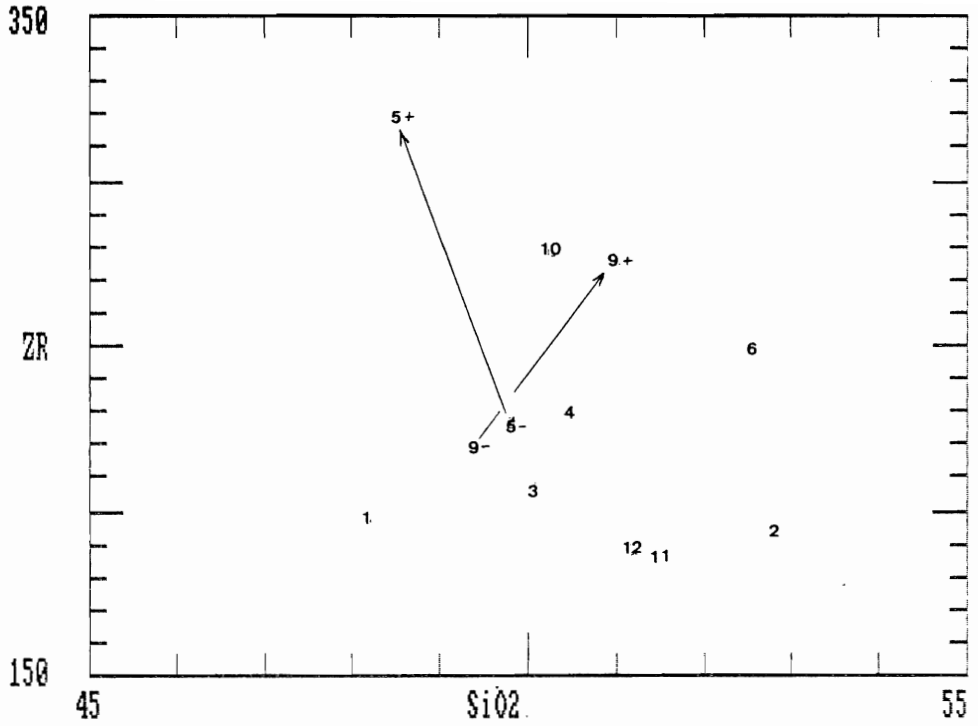

Figure 19c

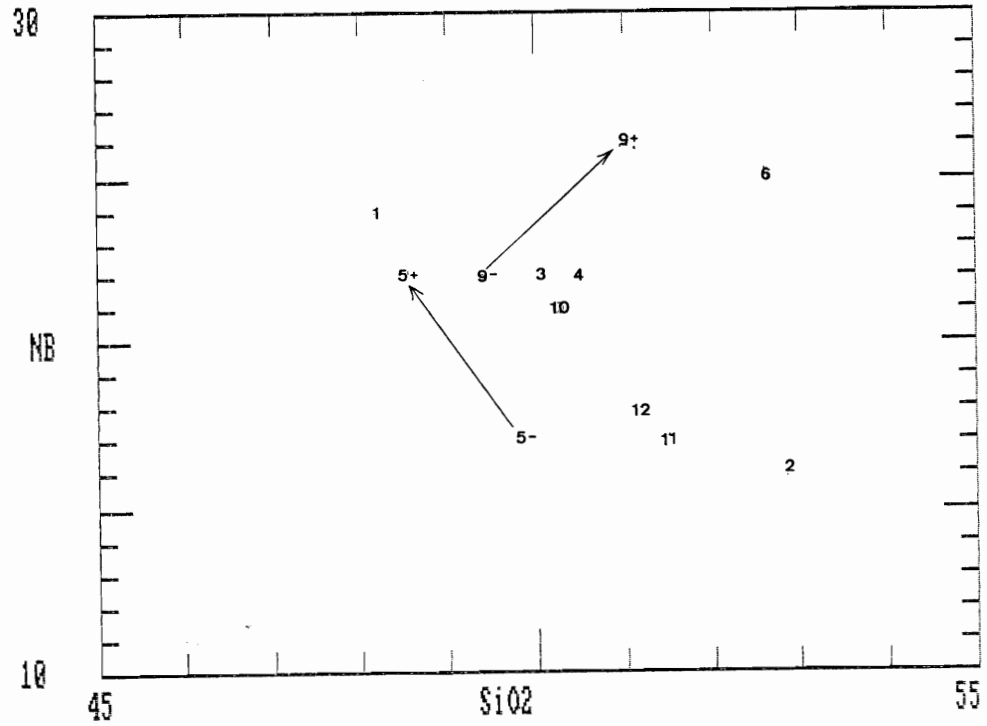

4.3 Comparison with Extrusive Rocks

Samples of basaltic volcanic rocks from the Strand Fiord Formation were collected by Marie-Claude Williamson during the 1983 field season. Two areas on Axel Heiberg Island were samples: Bunde Fiord and Strand Fiord (Figure 13). The purpose of this comparison is to determine whether there are any geochemical differences between the Lightfoot River dykes and the Strand Fiord Formation volcanics.

The elements chosen for comparison were: Y, Zr and Nb. These were chosen because they are known to be geochemically immobile and thus unaffected by weathering and alteration processes (ex. Zr, Humphris and Thompson 1978). In the two dykes for which interior and marginal samples were analyzed, these elements behaved in a manner consistent with increasing fractionation towards the centre of the dykes. This supports the assumption that they have not undergone major post-magmatic changes. A second reason for choosing these elements is that all three elements are incompatible with early formed crystals and thus are concentrated into the remaining melt. Since all three behave this way, the ratio between the three is going to remain fairly constant as crystallization proceeds, and there will be little or not expression of a fractionation trend on a ternary diagram of the three elements.

Analyses for ten dyke samples and averages for the volcanics at both Bunde Fiord and Strand Fiord are shown in Table 5.

TABLE 5

Y/2 - Zr/10 - Nb Values

For Dykes and Extrusives

SAMPLE	Y/2(ppm)	Zr/10(ppm)	Nb(ppm)
AX85-15*	22.5	25.0	25.0
AX85-19	22.5	27.6	26.0
AX85-20	19.5	22.0	22.0
AX85-26	23.0	27.8	21.0
AX85-31	21.0	22.7	17.0
AX85-35	29.5	31.9	22.0
AX85-40	25.5	22.9	22.0
AX85-43	21.5	20.7	22.0
AX85-46	20.5	19.5	16.0
AX85-48	21.0	19.8	24.0
Bunde Fiord** (average)	21.5	18.6	17.0
Strand Fiord (average)	19.5	18.8	18.0

A ternary plot of the analyses is shown in Figure 20. The results cluster in the central region of the plot showing that with respect to Y, Zr and Nb at least, the dykes and the extrusives are indistinguishable. The Harker diagrams on Figures 18 and 19 also show that the values for the extrusive rocks usually fall within the cluster of dyke values. CaO is the one exception (Figure 18d). In this case, the CaO value for the extrusives are slightly higher than the same value for the dykes. This is probably due to alteration affects and carbonate infilling of vesicles. The volcanics appear to be generally less differentiated that the dykes since they are slightly lower in Y, Zr, Nb and K_2O, (Figure 18f) elements that normally increase as fractionation occurs. This is probably due to the faster cooling of the extrusives or the lack of flow differentiation that may have occurred in the dykes. The lower TiO_2 values in the volcanics (Figure 18a) could be due to settling of early formed ilmenite and/or titaniferous augite.

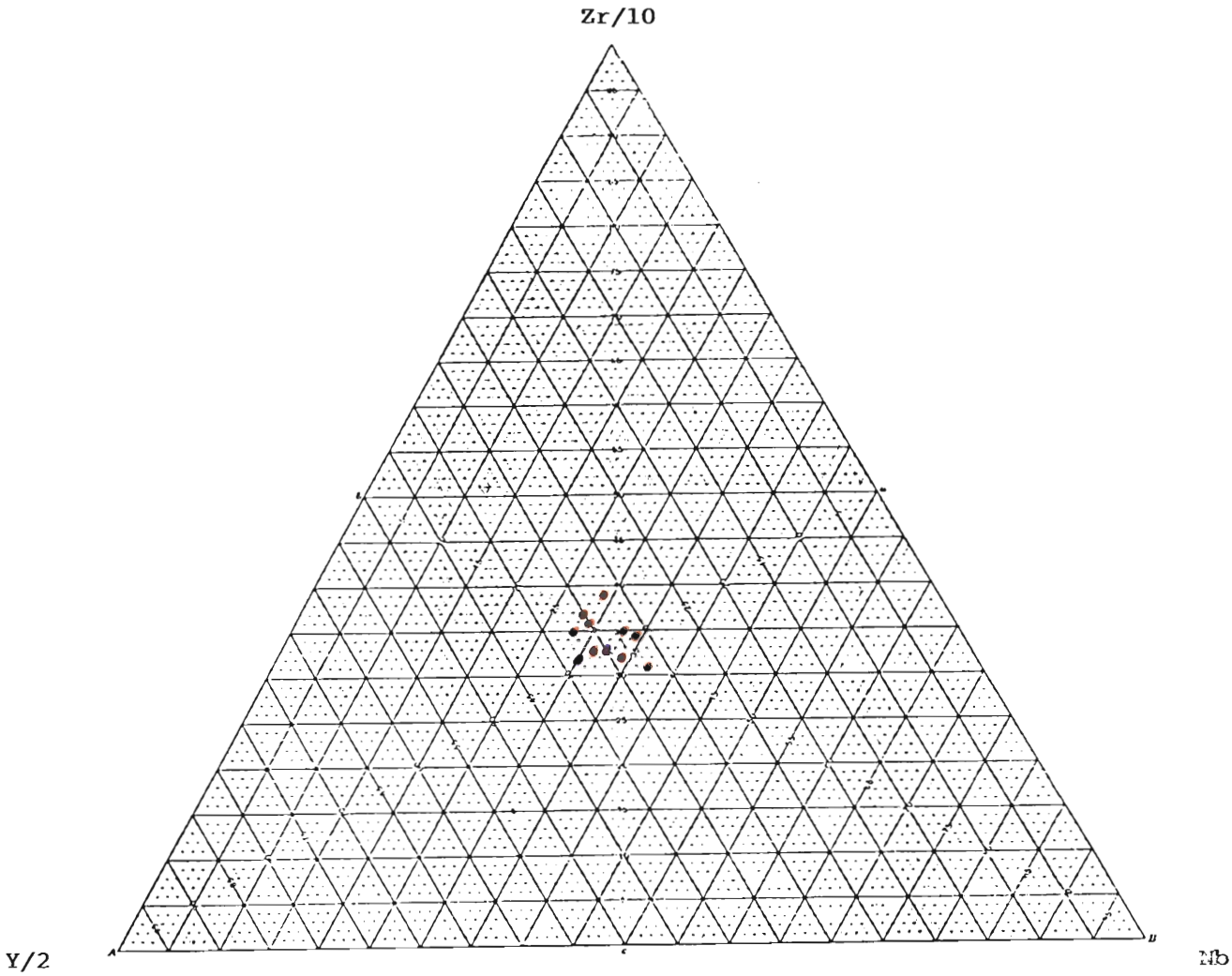

Figure 20: Zr/10 - Y/2 - Nb Ternary Plot for Dykes and Extrusives

*Dyke values in red, and extrusive values in blue.

CONCLUSIONS

CONCLUSIONS

Based on the data that is available, the author believes that there have been two major dyking episodes in the Sverdrup Basin. Bother of these events occurred during the Cretaceous since the trends are visible in all stratigraphic horizons prior to, and including the Lower Cretaceous. The first event produced Swarm A and Swarm B trends (Ø2Ø degrees to Ø5Ø degrees, and Ø6Ø degrees to Ø8Ø degrees respectively) throughout the entire basin. The second event produced Swarm C and Swarm D trends (31Ø degrees to 36Ø degrees, and ØØØ degrees to Ø2Ø degrees respectively). This event was restricted more to the northern end of the basin, and is believed to be the landward continuation of the Alpha Ridge complex on the basis of available evidence. The later event is not as prominent in the Upper Jurassic-Lower Cretaceous host rocks because these are found more towards the center of the basin, away from the area where the second dyking even is believed to be most prominent. The relative timing of these two events is not known at the present time.

The dykes in the Lightfoot River area of Axel Heiberg Island are representative of one of the dyking events in this area and are part of the north trending swarm. The petrography and mineralogy of the dykes in this area show that the dykes are tholeiitic in character with normative quartz. The dykes that have been sampled show normal crystal fractionation trends towards their interiors with some exceptions. These exceptions

are believed to have been caused by contamination from the country rock, xenoliths of country rock or alteration. However, a much broader study of this aspect is needed to determine the trends that are present within the dykes.

Comparison with the Strand Fiord volcanics show that on the basis of Y, Zr and Nb, the volcanics and the dykes are indistinguishable from each other. Comparison of the major and trace elements for bother groups show that they are similar in chemistry suggesting that they may be co-genetic. The Lightfoot River dykes are therefore possible candidates as feeders to the Strand Fiord volcanics. Alteration of these samples is often severe and may affect the comparison between the dykes and extrusives.

Future work is needed in several areas. First of all, a systematic sampling and dating is required to determine whether the north trending dyke sets are younger or older than the easterly trending A and B Swarms. Secondly, the comparison between the dykes and extrusives should be extended to isotopic studies to derive more definitive criteria as to a common ancestry.

PLATES

PLATE 1a

A Long Linear Dyke in the
Lightfoot River Area of Axel Heigberg Island

PLATE 1b

A Larger Dyke in the Field of the
Lightfoot River Area of Axel Heigberg Island

PLATE 2a

Flow Banding Along Dyke Margin
Lightfoot River Area Axel Heigberg Island

PLATE 2b

Felty Texture in Thin Section; also,
Phenocrysts of Plagioclase
(field of view 6.5 mm; sample # AX85-30

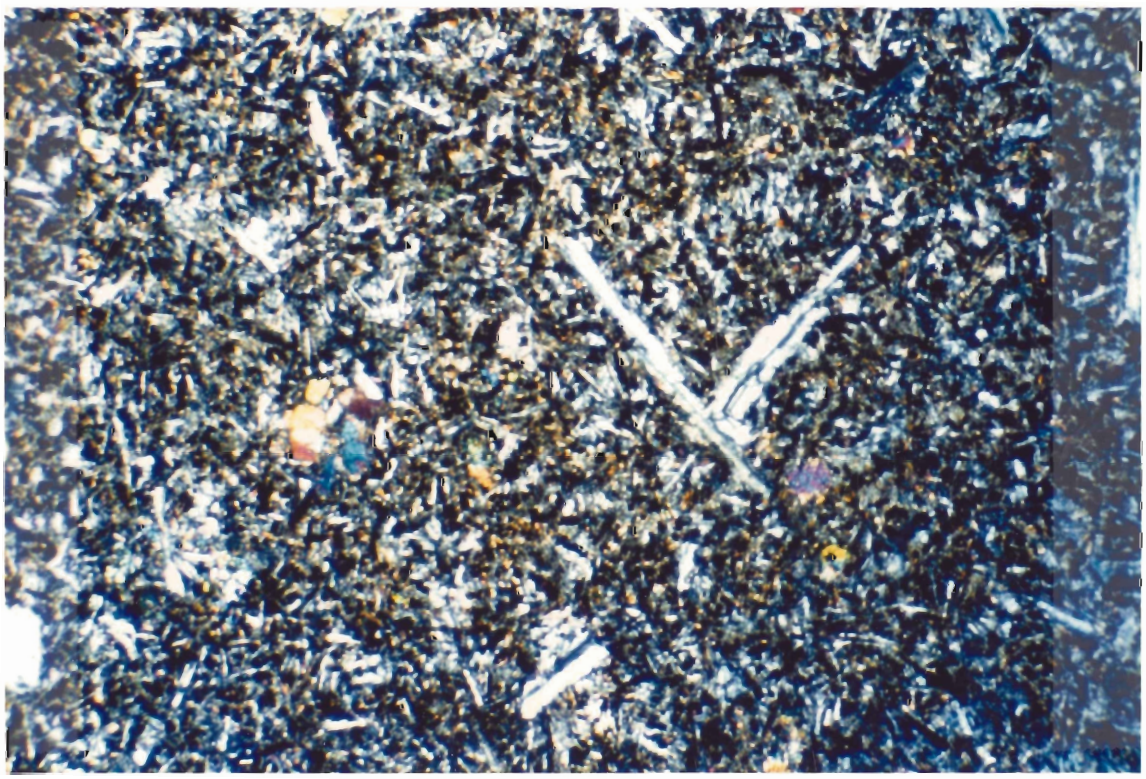

PLATE 3a

Intergranual Texture in Thin Section
(field of view 6.5 mm; sample # AX85-14)

PLATE 3b

Sericitized Plagioclase and Anhedral Clinopyroxene
(field of view 6.5 mm; sample # AX85-24)

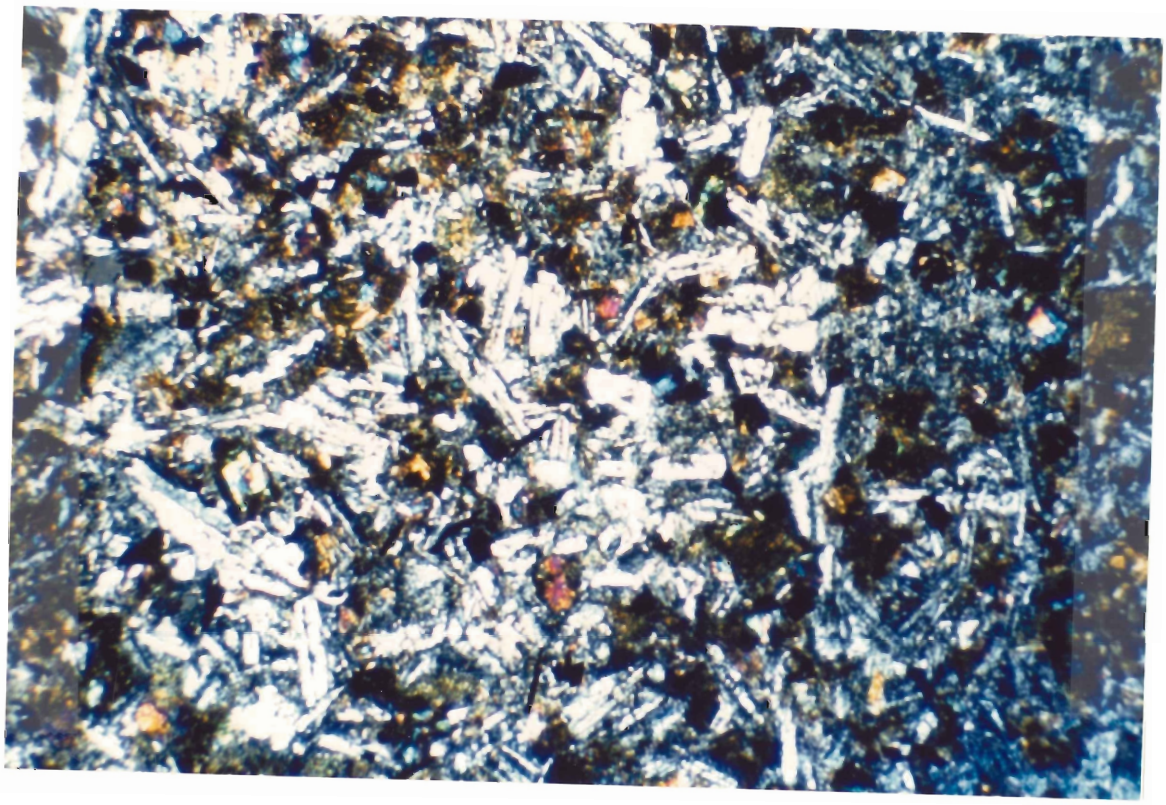

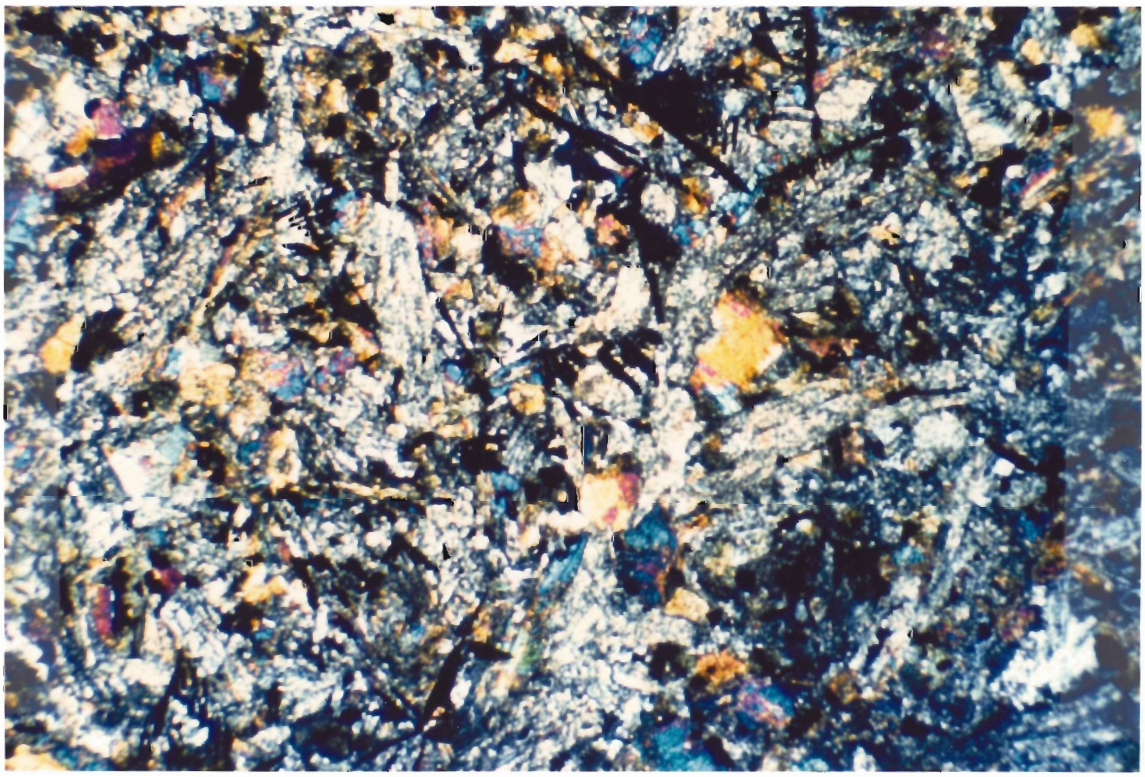

PLATE 4a

Tremolite and Altered Plagioclase in Thin Section
(field of view 6.5 mm; sample # AX85-35)

PLATE 4b

Ilmenite in Thin Section
(field of view 1.5 mm; sample # AX85-24)

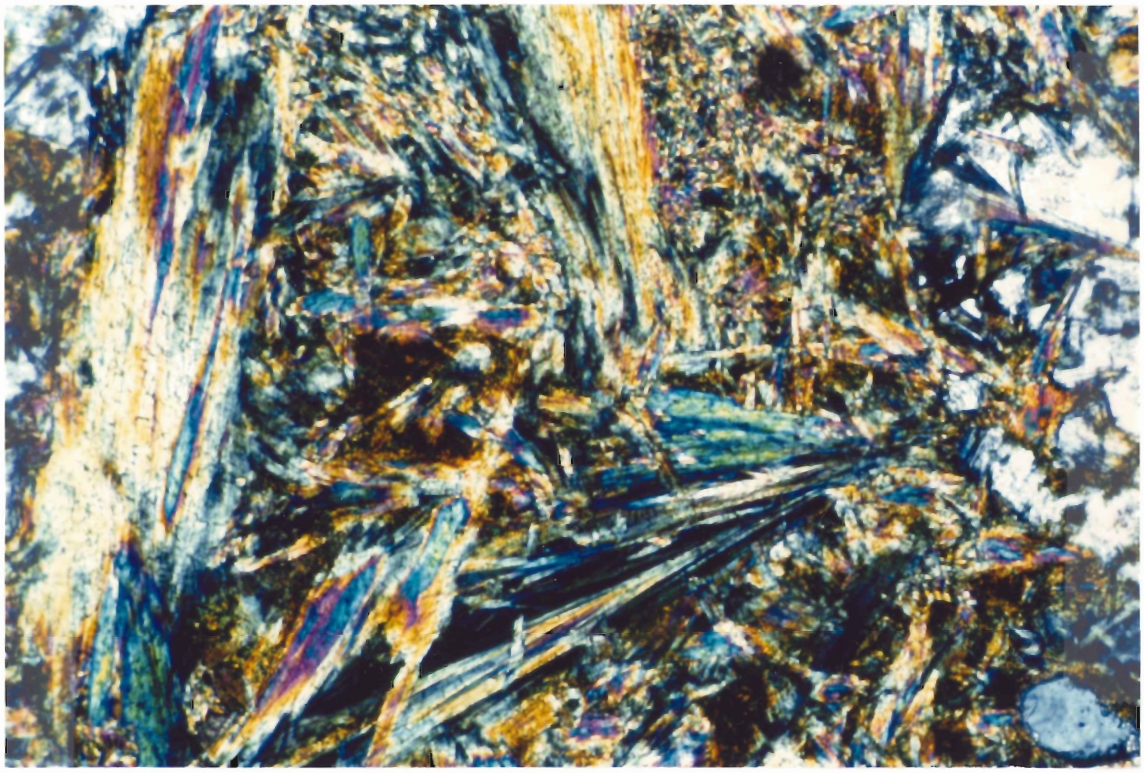

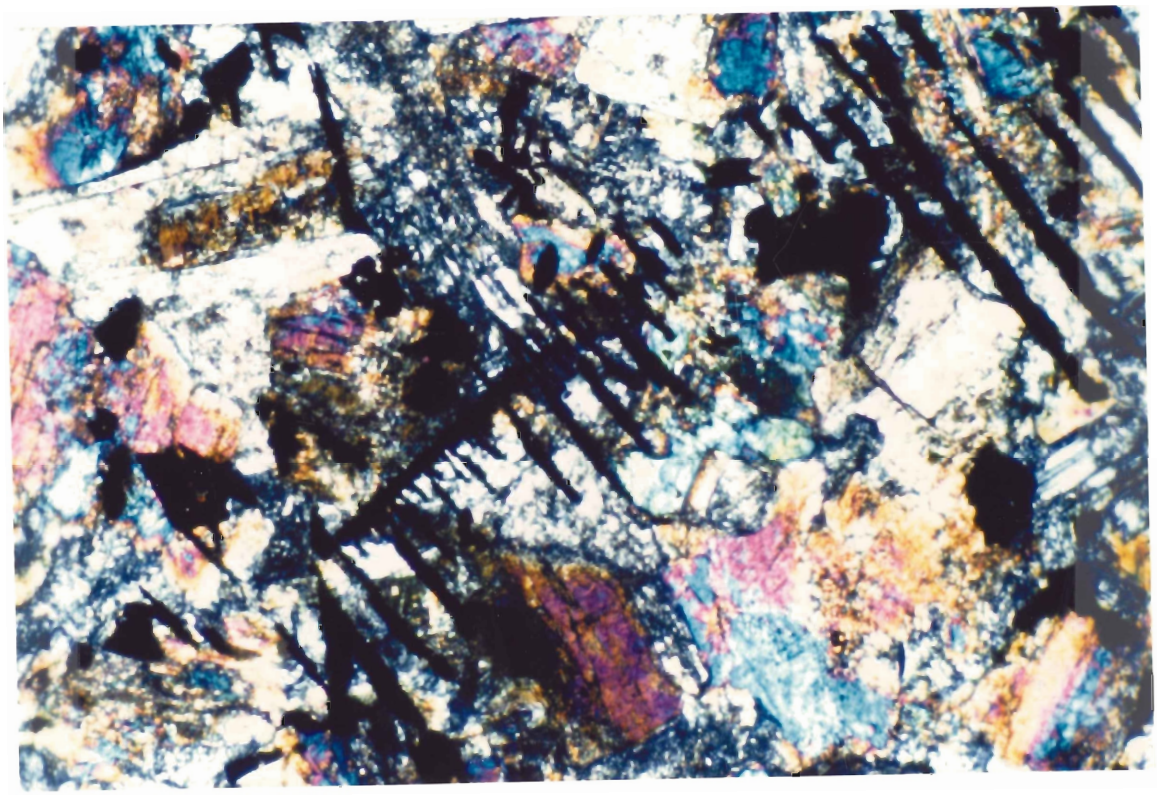

APPENDIX I

APPENDIX I

LIST OF GEOLOGICAL SURVEY OF CANADA
MAPS USED IN THIS THESIS

Map 1299A Middle Fiord District of Franklin

Map 1300A Eureka Sound South - District of Franklin

Map 1301A Strand Fiord - District of Franklin

Map 1302A Eureka Sound North - District of Franklin

Map 1303A Haig-Thomas Island - District of Franklin

Map 1304A Glacier Fiord - District of Franklin

Map 1305A Cape Stallworthy - District of Franklin

Map 1306A Tanquary Fiord - District of Franklin

Map 1308A Canon Fiord - District of Franklin

Map 1309A Otto Fiord - District of Franklin

Map 1310A Bukken Fiord - District of Franklin

Map 1311A Greely Fiord - District of Franklin

Map 1312A Baumann Fiord - District of Franklin

Map 1471A Amund Ringnes, Cornwall, and Haig Thomas Islands - District of Franklin

Map 4-1968 Ellef Ringnes Island - District of Franklin

All Scales 1:250,000 except Map 4-1968 which is 1:253,440

APPENDIX II

APPENDIX II

LIGHTFOOT RIVER DYKES

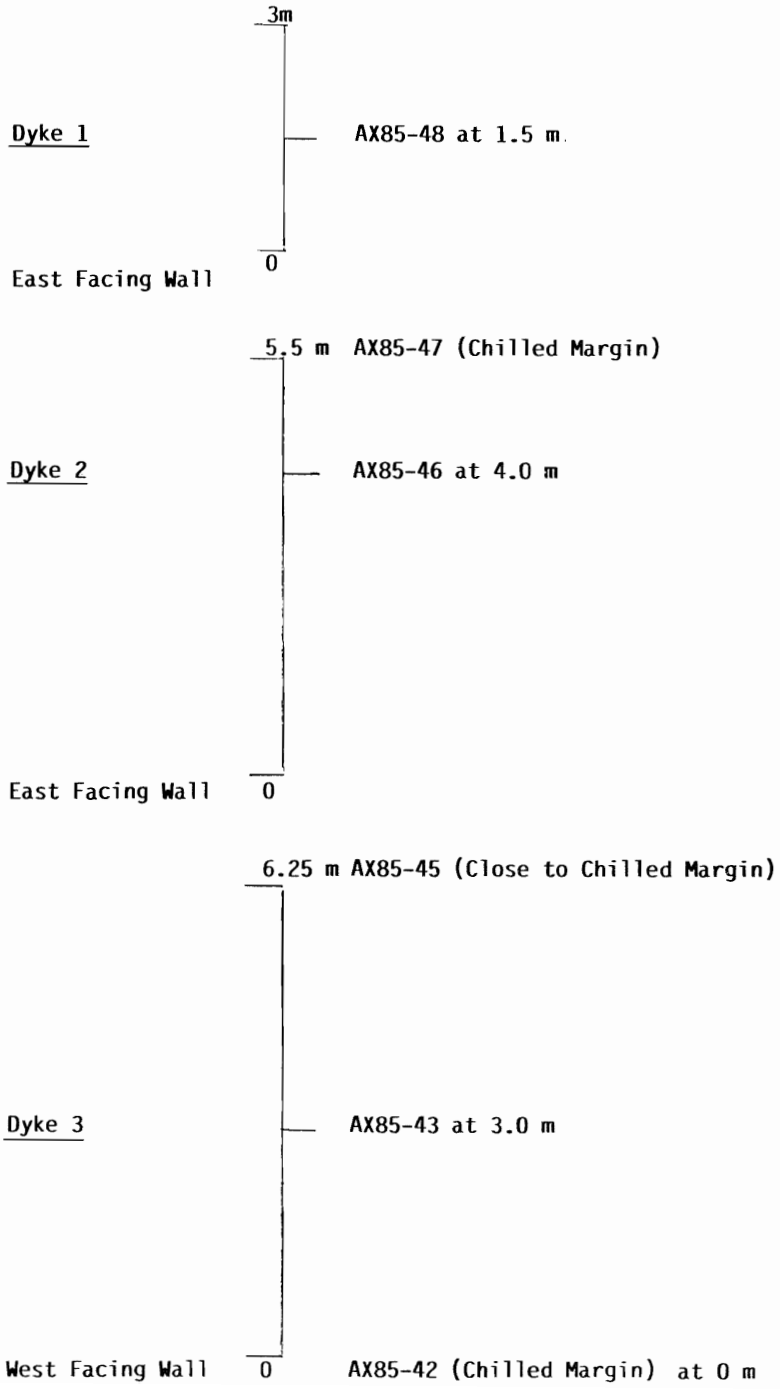

LIGHTFOOT RIVER DYKES

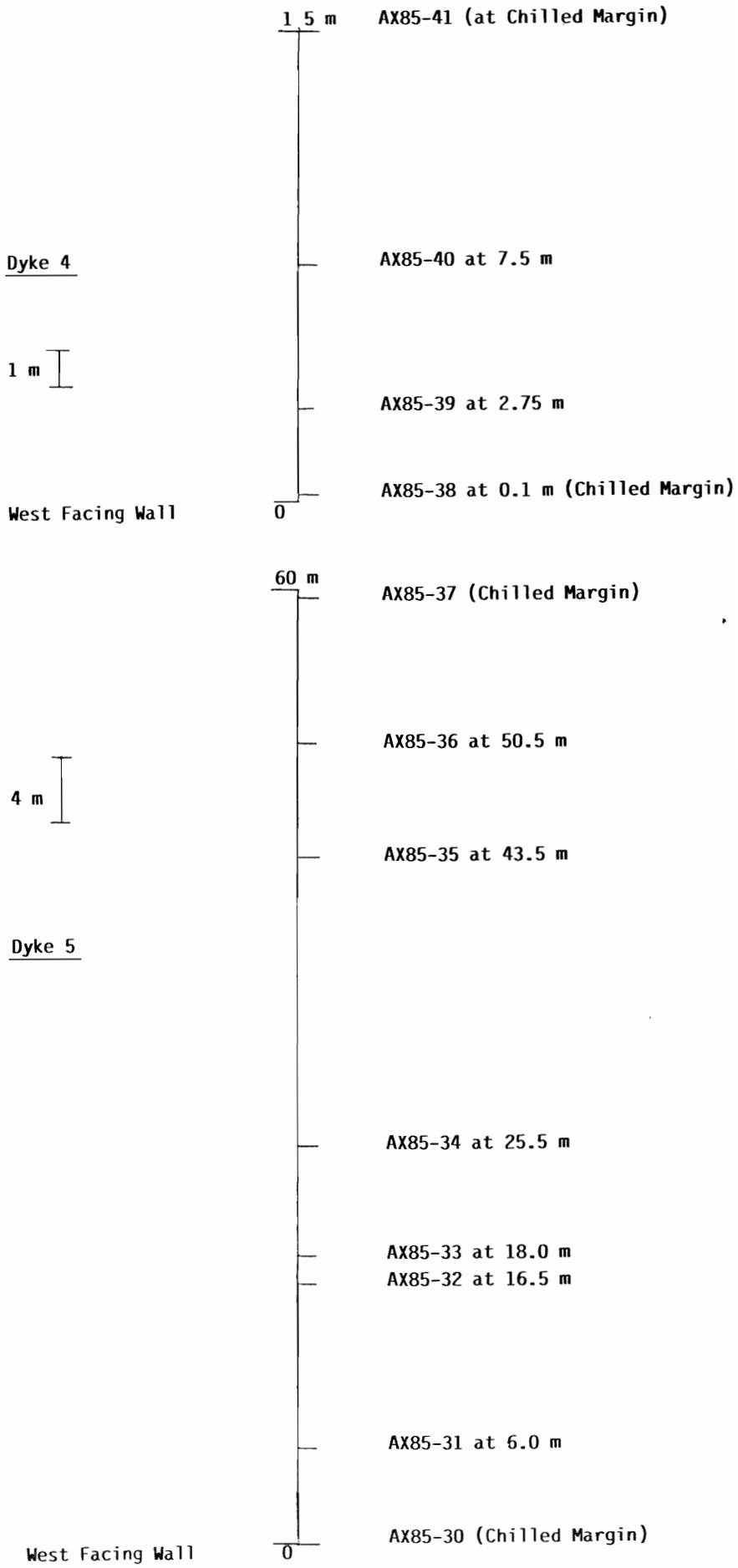

LIGHTFOOT RIVER DYKES

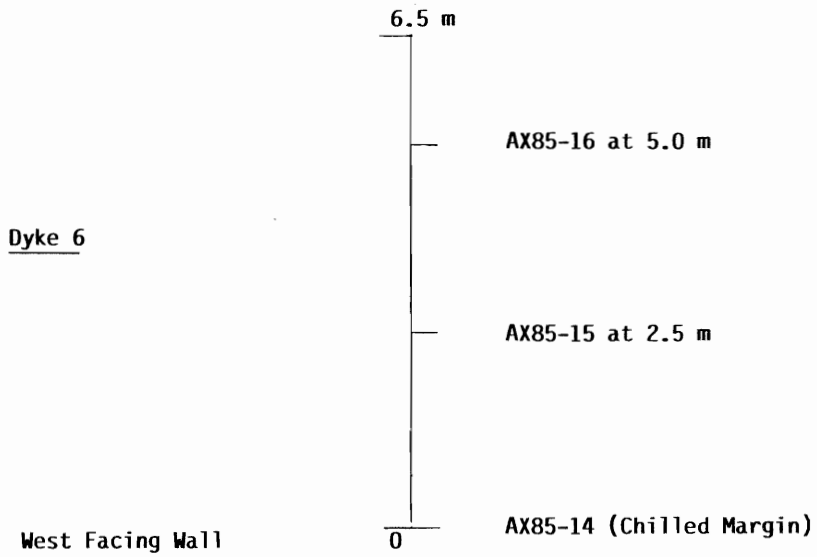

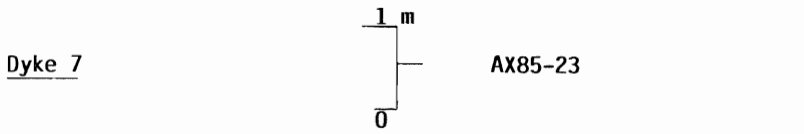

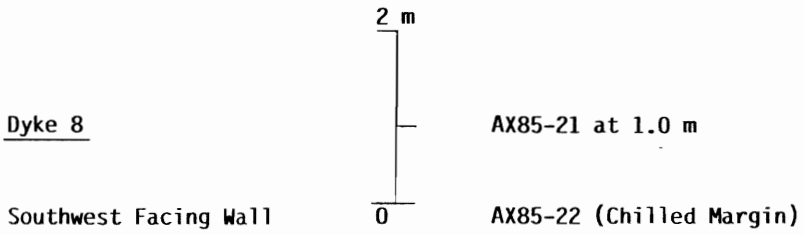

LIGHTFOOT RIVER DYKES

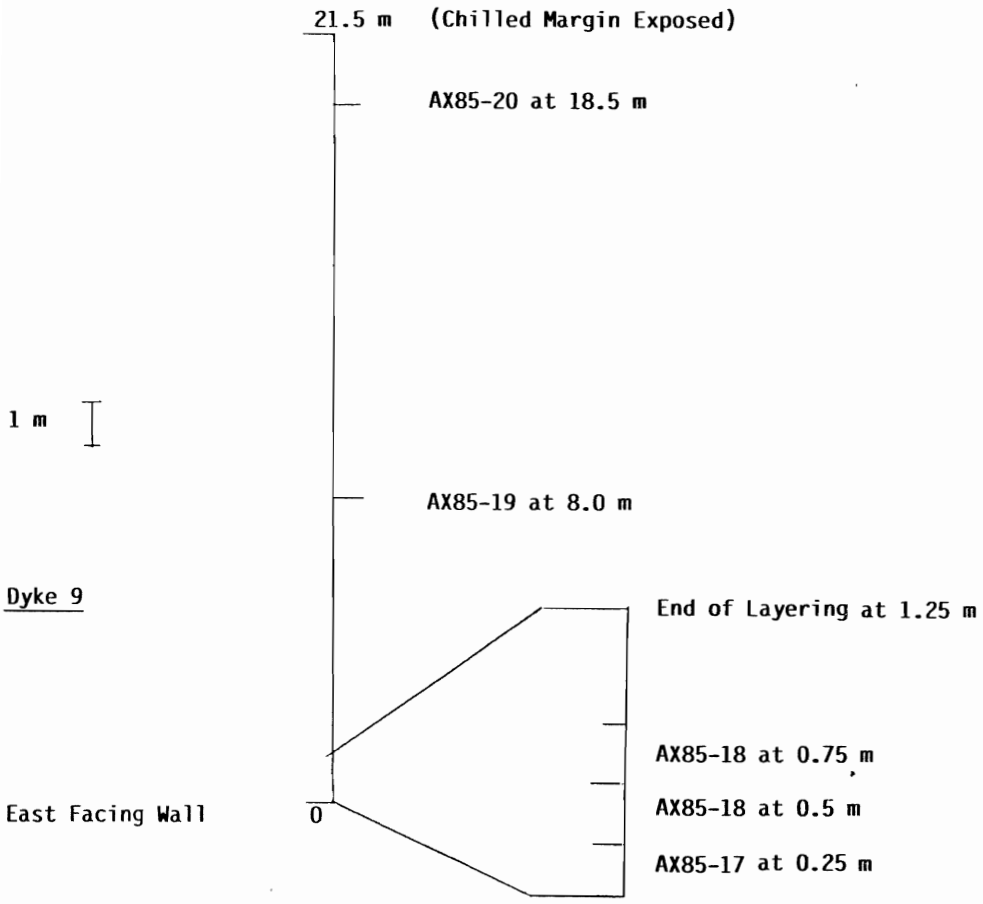

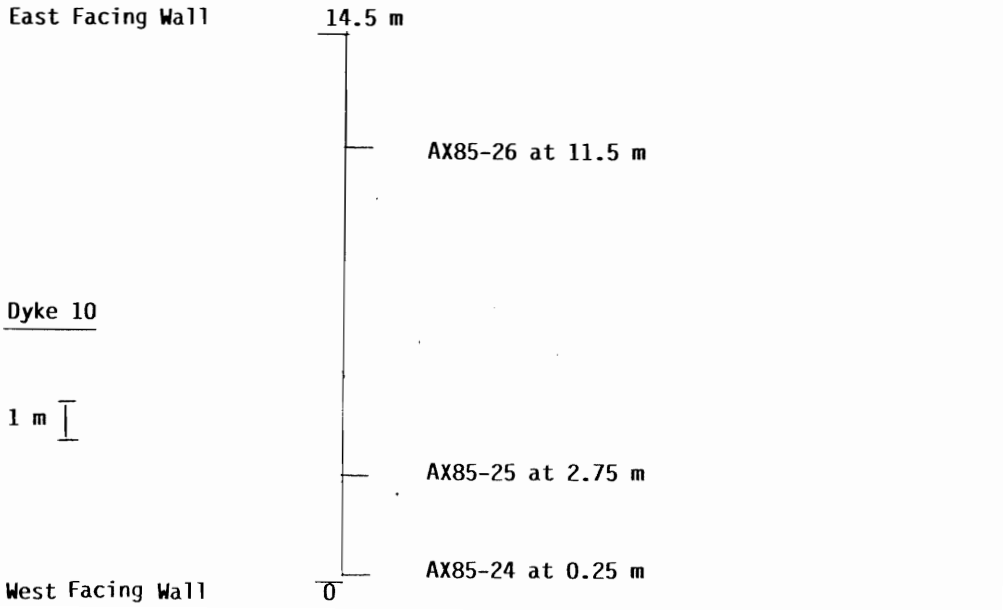

APPENDIX III

APPENDIX III

THIN SECTION SUMMARY

AX85-14

- 60% Plagioclase, An=42, euhedral crystals, 0.5 mm in size, weak alteration
- 10% Clinopyroxene, anhedral, 0.3 mm crystals, very strongly altered, reddish product
- 10% Opaques, euhedral 0.1 mm in size, octahedral cross-sections, centers very strongly corroded
- 15% Groundmass, fine grained alteration products, green color, possibly chlorite, minor quartz, very corroded
- Fine grained, holocrystalline, felty texture

AX85-15

- 60% Plagioclase, An=30, euhedral lath-shaped crystals, 2.0 mm long, moderate alteration
- 20% Clinopyroxene, anhedral, slightly corroded, included plagioclase laths
- 5% Opaques subhedral, octahedral and triangular cross-sections, some corrosion
- 5% Biotite, 0.5 mm long, mostly altered to chlorite, minor amounts of Quartz, very corroded and some calcite, replacing quartz (?) minor apatite
- Medium grained, ophitic texture

AX85-16

- 50% Plagioclase, grain size 1.0 mm, An=58, slight alteration
- 30% Clinopyroxene, anhedral, grain size 0.8 mm, strong alteration, reddish product
- 5% Opaques, euhedral, slightly corroded, 0.5 mm crystals
- 5% Chlorite, subhedral, 0.5 mm long crystals after biotite, small amount of biotite preserved, minor amounts of quartz, and calcite, quartz and very strongly corroded, some replacement by calcite
- Medium grained, subophitic texture

AX85-17

- 60% Plagioclase grain size 1.5 mm, very strongly altered, complete sericitization
- 20% Clinopyroxene, very strongly altered, red alteration product
- 5% Opaques, very corroded, grain size 0.3 mm, some biotite preserved
- Minor calcite, replaces plagioclase and quartz, minor quartz, very corroded, some apatite observed
- Subophitic texture, medium grained

AX85-18

- 60% Plagioclase, complete alteration to sericite
- 25% Clinopyroxene, 0.5 mm size, anhedral very corroded, red alteration product
- 10% Biotite 0.5 mm in size, partially altered to chlorite
- 5% Opaques - mostly ilmenite occurring in long (0.5 mm) crystals
- Minor quartz and calcite, quartz corroded, replaced by calcite
- Subophitic texture, medium grained

AX85-19

- 60% Plagioclase, completely altered to sericite
- 30% Clinopyroxene, subhedral 2.0 mm grain sizes retrograde altered to chlorite
- 5% Opaques, euhedral, grain size 0.25 mm, very corroded
- Minor minerals include quartz and calcite
- Coarse grained, subophitic texture

AX85-20

- 50% Plagioclase, grain size 1.5 mm, completely altered to sericite
- 30% Clinopyroxene, subhedral crystal size 1.0 mm, slightly retrograde altered to chlorite

- 5% Biotite, Ø.5 mm crystals, partially chloritized
- 5% Opaques, subhedral, slightly corroded, minor amounts of quartz, calcite, and apatite
- Medium grain sizes, subophitic to ophitic textures

AX85-24

- 6Ø% Plagioclase, completely sericitized
- 15% Clinopyroxene, anhedral, crystals Ø.5 mm long, corroded
- 5% Ilmenite, Ø.5 mm long, probably some magnetite also present
- 5% Chlorite, after clinopyroxene
- Minor quartz and apatite quartz slightly corroded
- Fine grained, intergranular texture

AX85-25

- 65% Plagioclase, 2.Ø mm in size, euhedral, An=5Ø strong sericitization
- 15% Clinopyroxene anhedral grain size 1.Ø mm, strong alteration
- 5% Quartz, anhedral grain size 1.Ø mm
- 5% Opaques, euhedral, grain sizes Ø.5 mm
- Coarse-grained ophitic texture

AX85-26

- 65% Plagioclase, completely sericitized, grain size 2.Ø mm
- 2Ø% Clinopyroxene, subhedral, 1.Ø mm grain size, strongly altered, red alteration product
- 5% Opaques, subhedral to euhedral, grain size 1.Ø mm, moderately corroded
- 5% Biotite, altered to chlorite
- Coarse grained, intergranular texture

AX85-3Ø

- 55% Plagioclase, occurs as euhedral phenocrysts (1.Ø mm) and in the groundmass, no alteration, An=44

- 20% Clinopyroxene occurs as phenocrysts (0.5 mm) and also in the groundmass, phenocrysts are euhedral to subhedral, no alteration

- 15% Opaques, very fine grain size, occurs in the ground mass, some may be ilmenite, no alteration

- Minor quartz is found in the groundmass

- Fine grained, porphyritic texture

AX85-31

- 65% Plagioclase euhedral, grain size 2.0 mm, strongly sericitized, a few unaltered grains give, An=32

- 20% Clinopyroxene, subhedral, grain size 1.0 mm, very strongly corroded

- 5% Opaques, euhedral, 1.5 mm grain size, possibly some ilmenite, very corroded

- 2% Biotite, very altered

- Coarse grained, intergranular texture

AX85-32

- 60% Plagioclase, completely altered, grain size 2.0 mm

- 30% Clinopyroxene, grain size 1.0 mm, moderately corroded

- 20% Calcite, replaces plagioclase and probably clinopyroxene, no Cpx observed

- 5% Opaques, 1.0 mm size, strongly corroded, minor quartz

- Texture would have been subophitic if clinopyroxene were still present

AX85-35

- 60% Plagioclase, An=51, strongly sericitized, grain size 3.0 mm

- 30% Clinopyroxene, 2.0 mm crystals, subhedral very altered, red alteration, some retrograde alteration to tremolite

- 2% Opaques, 1.5 mm across, euhedral, very corroded

- 2% Quartz, fine grained, showing subgrain development

- Minor minerals include calcite, and a lot of apatite

- Coarse grained, subophitic texture

AX85-36

- 65% Plagioclase An=50, slight alteration grain sizes up to 2.0 mm, euhedral crystals
- 25% Clinopyroxene, subhedral crystals up to 1.5 mm, slight corrosion
- 1% Biotite, slightly chloritized, crystals 0.5 mm
- 2% Opaques, up to 2.0 mm long, subhedral, extremely corroded
- Minor quartz and apatite, medium grained, ophitic texture

AX85-37

- 60% Plagioclase, fine grained microlitic, An content low
- 25% Clinopyroxene, anhedral, very altered, red alteration product
- 5% Opaques probably ilmenite
- 2% Biotite, minor quartz
- Fine grained, ophitic texture

AX85-38

- 50% Plagioclase, larger (2.0 mm) phenocrysts in a matrix of finer plagioclase laths (0.25 mm), extremely altered
- 30% Clinopyroxene, 0.25 mm crystals, very altered, reddish alteration product
- 5% Opaques, some ilmenite, crystals 0.5 mm long, moderately corroded
- 1% Biotite, 0.5 mm long, partly chloritized, minor quartz and apatite, quartz very corroded, calcite replacing quartz
- Fine grained, subophitic (?) texture

AX85-40

- 65% Plagioclase, An=48, subhedral crystals, 1.5 mm in size, strongly altered
- 20% Clinopyroxene, anhedral, 1.0 mm in size, moderate alteration, reddish product

- 5% Opaques, euhedral, Ø.5 mm in size, slight corrosion
- Minor quartz (corroded) and apatite
- Medium grained, subophitic texture

AX85-41

- 1Ø% Plagioclase phenocrysts up to 1.Ø mm euhedral crystals, slightly altered
- 2% Clinopyroxene subhedral, Ø.3 mm, some alteration
- 2% Opaques subhedral, Ø.3 mm in size, slight corrosion
- Minor apatite observed within the plagioclase phenocrysts
- Groundmass includes extremely find grained plagioclase, clinopyroxene and opaques
- Fine grained, porphyritic texture with aligned phenocrysts - flow banding (?)

AX85-42

- 6Ø% Plagioclase up to 1.5 mm in size, slightly altered
- 15% Clinopyroxene, anhedral up to 1.Ø mm in size, altered, red alteration product, some crystals show zoning
- 5% Opaques, subhedral, up to Ø.5 mm, very corroded
- Minor quartz, no apatite
- Fine grained, porphyritic texture

AX85-43

- 65% Plagioclase, completely altered to sericite, grain sizes up to 2.Ø mm
- 15% Clinopyroxene, anhedral crystals, up to 1.Ø mm, some altered to chlorite
- 1Ø% Opaques up to 1.Ø mm, very corroded
- Minor quartz and calcite, very little apatite
- Medium grained, intergranular texture

AX85-44

- 9Ø% Calcite, replaces entire rock

- 5% Plagioclase, severely altered, almost unrecognizable

- 1% Clinopyroxene, almost completely destroyed

- 2% Opaques, strongly corroded

AX85-45

- 60% Plagioclase, subhedral crystals up to 1.5 mm long, strongly sericitized

- 20% Clinopyroxene, subhedral, strong alteration, red alteration product, grain size 1,0 mm

- 5% Opaques, euhedral, moderately corroded

- Minor quartz, calcite and apatite

- Medium grained subophitic texture

AX85-46

- 60% Plagioclase, An=38, subhedral, up to 1.5 mm long, slight alteration, some grains show zoning

- 25% Clinopyroxene, subhedral crystals, 0.5 mm in size, very little alteration

- 3% Opaques, up to 1.0 mm in size, euhedral, some corrosion

- 2% Chlorite, 0.5 mm, after biotite and clinopyroxene

- Minor quartz, calcite, very little apatite

- Medium grained, ophitic texture

AX85-47

- 60% Plagioclase, anhedral, 1.0 mm in size, completely altered to sericite

- 20% Clinopyroxene, anhedral, 0.5 mm in size, slightly altered, red product

- 5% Opaques, euhedral, up to 0.5 mm in size, slightly corroded

- 1% Chlorite, anhedral after biotite

- Minor quartz, no apatite

- Fine grained, ophitic texture

AX85-48

- 65% Plagioclase, subhedral, up to 2.0 mm, completely altered
- 15% Clinopyroxene, anhedral up to 0.5 mm, very strongly altered
- 5% Opaques, euhedral, 0.5 mm in size, moderately corroded
- Minor quartz and apatite, calcite replaces plagioclase
- Medium grained, ophitic texture

BIBLIOGRAPHY

BIBLIOGRAPHY

1. Arctic Islands: Davis Strait to Beaufort Sea; Published by the Hydrographic Service, Department of Fisheries and Oceans, Government of Canada, 1980. (Scale 1:4,000,000).

2. Balkwill, H.R. 1983, Sverdrup Basin - Eurekan Orogeny tectogenesis of a passive margin basin (abs.) Geol. Assoc. Can./Min. Assoc. Can/Can. Geophys. Union Joint Annual Meeting, Program with Abstracts; pg. A3.

3. Balkwill, H.R. 1983, Geology of Amund Ringnes, Cornwall, and Haig-Thomas Islands, District of Franklin; Geological Survey of Canada, Memoir 390, 76 pgs.

4. Balkwill, H.R. 1978, Evolution of Sverdrup Basin, Arctic Canada; AAPG Bull., Vol. 62, No. 6, pgs. 1004-1028.

5. Balkwill, H.R. & Fox, F.G., 1982, Incipient rift zone, western Sverdrup Basin, Arctic Canada, Can. Soc. Petrol. Geol., Mem. 8, pgs. 171-187.

6. Balkwill, H.R., Wilson, D.G. & Wall, J.H. 1977, Ringnes Formation (Upper Jurassic), Sverdrup Basin, Canadian Arctic Archipelago, Bull. Can. Petrol. Geol., Vol. 25, pgs. 1115-1144.

7. Barker, D.S. 1983 Igneous Rocks, Prentice - Hall, Inc. 417 pgs.

8. Blackadar, R.G., 1964, Basic intrusions of the Queen Elizabeth Islands, District of Franklin Geol. Surv. Can. Bull. 97, 37 pgs.

9. Best, M.B. 1982, Igneous and Metamorphic Petrology, W.H. Freeman and Company, 630 pgs.

10. Chart #9, Information and Activity, Canada, North of 60 degrees, 1971, published by Department of Indian Affairs and Northern Development (Mapping and Cartigraphy).

11. Clarke, D.B., 1969, Tertiary basalts of the Baffin Bay area. PhD Thesis, University of Edinburgh, 122 pgs. (unpublished document)

12. Clarke, D.B., 1970, Tertiary basalts of Baffin Bay: possible primary magma from the mantle. Contrib. Mineral Petrol Vol. 25, pgs. 203-24.

13. Clarke, D.B., 1975, Tertiary basalts dredged from Baffin Bay; Can J. Earth Sci Vol. 12, pgs. 1396-1405.

14. Clarke, D.B., Muecke, G.K., and Pe-Piper, G., 1983, The lamprophyres of Ubekendt Ejland, West Greenland: products of renewed partial melting or extreme differentiation? Contrib Mineral Petrol Vol. 83, pgs. 117-127.

15. Embry, A.F., 1982, The Upper Triassic-Lower Jurassic deltaic complex of the Sverdrup Basin. Can. Soc. Pet. Geol., Mem. 8, pgs. 189-217.

16. Embry, A.F., 1983a, Stratigraphic subdivision of the Heiberg Formation, eastern and central Sverdrup Basin. Geol. Surv. Can. paper 83-1B, pgs. 205-213.

17. Embry, A.F., 1983b, The Heiberg Group, western Sverdrup Basin. Geol. Surv. Can. Paper 83-1B, pgs. 381-389.

18. Embry, A., and Klovan, J.E., 1976, The Middle-Upper Devonian clastic wedge of the Franklinian geosyncline: Bull. Can. Petrol. Geol., Vol. 24, pgs. 485-639.

19. Humphris, S.E. and Thompson, G., 1978, Trace element mobility during hydrothermal alteration of oceanic basalt, Geochim. Cosmochim, Acta, Vol. 42, pgs. 127-136.

20. Irvine, T.N., and Baragar, W.R.A., 1971, A guide to the chemical classification of the common volcanic rocks, Can. J. Earth Sci., Vol. 8, pgs. 523-548.

21. Jackson, H.R., 1985, Nares Strait - a suture zone: geophysical and geological implications Tectonophysics, Vol. 114, pgs. 11-28.

22. Jackson, H.R., Forsyth, D.A. and Johnson, G.L. (in press) Oceanic affinities of the Alpha Ridge, Arctic Ocean.

23. Jackson, K.C. and Halls, H.C., 1983, A paleomagnetic study of igneous rocks of the Sverdrup Basin, Canadian Arctic Archipelago (Abstract), GAC-MAC-CGU, 1983 Joint Meeting Victoria, Program with Abstracts, 8, 84 pgs.

24. Kerr, W.M., 1980, A Plate tectonic contest in Arctic Canada, Geological Association of Canada Special Paper 20 pgs. 457-486.

25. Larochelle, A., Black, R.F., and Wanless, R.K., 1965, Paleomagnetism of the Isachsen diabasic rocks: Nature, Vol. 208, no. 5006, pg. 179.

26. Monahan, D. and Johnson, G.L., 1982, Physiography of Nares Strait: importance to the origin of the Wegener Fault, Meddr Gronland, Geosci Vol. 8, pgs. 53-64.

27. Osadetz, K.G., 1982, Eurekan structures of the Ekblaw Lake area, Ellesmere Island Canada, Can Soc. Petrol. Geol. Mem. 8, pgs. 219-232.

28. Osadetz, K.G. and Moore, P.R. (in press), Basic volcanics in the Hassel Formation (Mid-Cretaceous) and associated intrusives, Ellesmere Island, District of Franklin, Northwest Territories, Canada.

29. Ostenso, N.A. and Wold, R.J., 1977, A seismic and gravity profile across the Arctic Ocean basin, Tectonophysics, Vol. 37, pgs. 1-24.

30. Ricketts, B., Osadetz, K.G., and Embry, A.F., 1985, Volcanic style in the Strand Fiord Formation (Upper Cretaceous), Axel Heiberg Island, Canadian Arctic Archipelago, Polar Research 3 n.s., pgs. 107-122.

31. Sobczak, L.W., 1982, Fragmentation of the Canadian Arctic Archipelago, Greenland, and surrounding oceans, Meddr Gronland, Geosci. Vol. 8, pgs. 221-236.

32. Sobczak, L.W., 1963, Regional gravity survey of the Sverdrup Islands and vicinity with Map: No. 11 - Sverdrup Islands, 19 pgs.

33. Sobczak, L.W. and Weber, J.R., 1970, Crustal structure of the Queen Elizabeth Islands and polar continental margin, Canada-Mem. Am Ass. Petrol. Geol. Vol. 19, pgs. 517-525.

34. Sweeney, J.F., 1984, Arctic tectonics - what we know today, Geos. 1984 Vol. 4.

35. Sweeney, J.F., Irving, E., and Geuer, J.W., 1978, Evolution of the Arctic Basin in Sweeney, J.F., ed. Arctic Geophysical Review, Earth Physics Branch Canada, Vol. 45, no. 4, pgs. 91-100.

36. Thorsteinsson, R., 1974, Carboniferous and Permian Stratigraphy of Axel Heiberg Island and Western Ellesmere Island, Canadian Arctic Archipelago - Bull. Geol. Surv. Can. Vol. 224, 115 pgs.

37. Thorsteinsson, R., 1971a, Middle Fiord, District of Franklin: Can Geol. Surv. Map 1299a, scale 1:250,000.

38. Thorsteinsson, R., 1971b, Eureka Sound North, District of Franklin: Can. Geol. Survey Map 1302 A, Scale 1:250,000.

39. Thorsteinsson, R. and Tozer, E.T., 1970, Geology of the Arctic Archipelago in Douglas, R.J.W., ed. Geology and Economic Minerals of Canada, Chapter X, Economic Geology Report No. 1, Fifth Edition: Geol. Surv. Can. p. 548-590.

40. Thorsteinsson, R. and Tozer, E.T., 1960, Summary account of the structural history of the Canadian Arctic Archipelago since Precambrian time - Pap. Geol. Surv. Can. Vol. 60-7, 23 pgs.

41. Trettin, H.P., Frisch, T.O., Sobczak, L.W., Weber, J.R., Niblett, E.R., Law, L.K., DeLaurier, J.M., and Whitham, K., 1972, The Innuitian Province: Geol. Assoc. Canada Spec. Paper 11, pgs. 83-179.

42. Trettin, H.P., and Hills, L.V., 1966, Lower Triassic tar sands of northwestern Melville Islands, Arctic Archipelago: Can. Geol. Sur. Paper 66-34, 122 pgs.

43. Williamson, M-C., 1985, Progress Report, April, 1985.